arXiv:1208.4234v1 [cond-mat.str-el] 21 Aug 2012

# Wilson-Loop Characterization of Inversion-Symmetric Topological Insulators

A. Alexandradinata,[1] Xi Dai,[2] and B. Andrei Bernevig[1]
[1]*Department of Physics, Princeton University, Princeton, NJ 08544*
[2]*Beijing National Laboratory for Condensed Matter Physics and Institute of Physics,*
*Chinese Academy of Sciences, Beijing 100080, China*
(Dated: August 22, 2012)

In the context of translationally-invariant insulators, Wilson loops describe the adiabatic evolution of the ground state around a closed circuit in the Brillouin zone. We propose that the Wilson-loop eigenspectrum provides a complete characterization of the inversion-symmetric topological insulator. Through the Wilson loop, we formulate a criterion for nontriviality that indicates a $\mathbb{Z}$ classification of 1D inversion-symmetric insulators. If the ground-state wavefunctions at momenta 0 and $\pi$ transform under different representations of inversion, we find that a subset of the Wilson-loop eigenvalues are robustly quantized to -1; we identify the number of -1 eigenvalues as a topological index $N_{(-1)} \in \mathbb{Z}$. Physical interpretations of $N_{(-1)}$ are provided in holonomy and in the geometric-phase theory of polarization. In addition, we identify $N_{(-1)}$ with the number of protected boundary modes in the entanglement spectrum. In 2D, we identify a relative winding number $W$ which provides a $\mathbb{Z}$ classification of 2D inversion-symmetric insulators. For insulators with nonzero $W$, their Wilson-loop eigenspectra exhibit spectral flow that is protected only by inversion symmetry. Hence, $W$ is the inversion-analog of the first Chern class $C_1$ (for charge-conserving insulators) and the $\mathbb{Z}_2$ invariant $\Xi$ (for time-reversal invariant insulators). Finally, we establish relations between the topological invariants $(W, C_1, \Xi)$ and the Wilson-loop eigenvalues at symmetric lines in the 2D Brillouin zone.

PACS numbers: 74.20.Mn, 74.20.Rp, 74.25.Jb, 74.72.Jb

There is strong evidence supporting the view that the topological properties of a condensed-matter system are encoded in its ground state alone.[1–48] From this point of view, a translationally-invariant topological insulator[49] is characterized by a local gauge redundancy – its ground state is invariant under a unitary transformation in the subspace of occupied Bloch bands. Since all topological quantities must be invariant under this transformation, a natural object to investigate is the eigenspectrum of a Brillouin-zone Wilson loop ($\mathcal{W}$).[50–59] In the context of topological insulators, $\mathcal{W}$ describes the adiabatic, unitary evolution of $n_{occ}$ occupied Bloch bands around a closed circuit in the BZ. More precisely, $\mathcal{W}$ is defined as the path-ordered exponential of the Berry-Wilczek-Zee connection $C_k^{nm}(k_\mu) = \int d^dr\; u_k^{n*}(r)\, \partial_{k_\mu}\, u_k^m(r)$:[60,61]

$$\mathcal{W} = \mathrm{T}\,\exp\big[\,\text{-}\int dk_\mu\; C_k(k_\mu)\,\big], \qquad (1)$$

where $u_k^n(r) = u_k^n(r+R)$ is the periodic component of the Bloch wave. Here, $T$ denotes path-ordering and $k_\mu \in \{k_1, \dots, k_d\}$ denote momenta components in a $d$-dimensional BZ. As Zak demonstrated for $n_{occ} = 1$, the Abelian $\mathcal{W}$ is nothing less than the Berry-phase factor acquired by a Bloch wave along a cyclic evolution.[62,63] For general $n_{occ}$, (1) forms a matrix representation of a holonomy, *i.e.*, a parallel transport map; holonomies are known to have diverse applications in physics.[64–66]

The Wilson loop is known to provide a characterization of the time-reversal-breaking Chern insulator[49] and the time-reversal-symmetric (TRS) $\mathbb{Z}_2$ insulator.[57,67] In this paper, we employ the Wilson loop to study topological insulators with the simplest point-group symmetry: inversion.[46–48,68,69] Specifically, we analyze how inversion ($\mathcal{I}$) symmetry manifests in the $\mathcal{W}$-eigenspectrum of Chern insulators and $\mathbb{Z}_2$ insulators. In addition, we identify topological invariants that are protected only by $\mathcal{I}$ symmetry, and offer physical interpretations of these invariants in holonomy and in the geometric-phase theory of polarization.

We first present a summary of our findings. For the 1D $\mathcal{I}$-symmetric insulator, we derive a mapping between the $\mathcal{I}$ eigenvalues of the ground state and the eigenvalues of $\mathcal{W}$; in particular we show that the only allowed $\mathcal{W}$-eigenvalues are +1, -1 and complex-conjugate pairs; in Tab. I, we show an example of this mapping for a generic insulator with four occupied bands. We propose that the nontrivial $\mathcal{I}$-symmetric insulator is characterized by $\mathcal{W}$-eigenvalues fixed at -1; the number ($N_{(-1)}$) of degenerate eigenstates at -1 is a $\mathbb{Z}$ topological index, which has the following physical interpretations: (i) if we adiabatically transport an insulating ground state with $n_{occ}$ occupied bands around the 1D BZ, $N_{(-1)}$ of $n_{occ}$ electrons pick up Berry phases of $\pi$ (ii) in a periodic 1D lattice, $N_{(-1)}$ number of maximally-localized Wannier functions localize in the middle of each adjacent pair of atomic sites; we call this the mid-bond site. Moreover, we shall identify $N_{(-1)}$ as the number of protected mid-gap modes in the entanglement spectrum[5,70] of an inversion-symmetric insulator.[48,71] The presence of these mid-gap modes ensure that the entanglement entropy can never be tuned to zero by any gap- and symmetry-preserving transformation – this has been proposed as a criterion for nontriviality that unifies all known topological insulators.[48] While these mid-gap modes are boundary states, the Wilson loop is a bulk property – together they provide consistent and complementary characterizations of the $\mathcal{I}$-symmetric insulator.

| $\mathcal{I}$ eigenvalues at $\{0,\pi\}$ | $\mathcal{W}$-spectrum |
|---|---|
| $\{(++++)\ (++++)\}$ | $[++++]$ |
| $\{(++++)\ (+++-)\}$ | $[+++-]$ |
| $\{(++++)\ (++--)\}$ | $[++--]$ |
| $\{(++++)\ (+---)\}$ | $[+---]$ |
| $\{(++++)\ (----)\}$ | $[----]$ |
| $\{(+++-)\ (+++-)\}$ | $[\lambda\lambda^*++]$ |
| $\{(+++-)\ (++--)\}$ | $[\lambda\lambda^*+-]$ |
| $\{(+++-)\ (+---)\}$ | $[\lambda\lambda^*--]$ |
| $\{(++--)\ (++--)\}$ | $[\lambda\lambda^*\ \mu\mu^*]$ |

TABLE I. For an insulator with four occupied bands, we tabulate the $\mathcal{I}$ eigenvalues of the occupied bands at symmetric momenta $\{0,\pi\}$ and the corresponding $\mathcal{W}$-spectrum. We collect the $\mathcal{I}$ eigenvalues $\xi_i$ at each symmetric momenta into $(\xi_1\,\xi_2\,\xi_3\,\xi_4)$. $+$ $(-)$ refers to an eigenvalue of +1 (-1); $\lambda\,\lambda^*$ and $\mu\,\mu^*$ refer to complex-conjugate-pair $\mathcal{W}$-eigenvalues.

For the 2D $\mathcal{I}$-symmetric insulator, we represent the quantum-mechanical electron density by a lattice of classical line charges. These line charges extend in $\hat{y}$ in the manner of a 1D Bloch wave, but localize in $\hat{x}$ in the manner of a 1D Wannier function (WF), hence we call them hybrid WF's. By evaluating Wilson loops at constant $k_y$, the phases $\{\vartheta(k_y)\}$ of the $\mathcal{W}$-spectrum represent the $\hat{x}$-coordinates of these hybrid WF's; we refer to them as Wannier centers.[72–78] Upon applying an electric field in $\hat{y}$, $k_y$ may be thought of as a time-coordinate in the adiabatic evolution. $\{\vartheta(k_y)\}$ represent the real-space trajectories of the Wannier centers in $\hat{x}$, as a function of time $k_y$. We identify the first Chern class, $C_1 \in \mathbb{Z}$, as the net $\hat{x}$-translation of the Wannier centers in a period $2\pi$;[79–85] the TR invariant, $\Xi \in \mathbb{Z}_2$, is the change in time-reversal polarization over a half-period; $\Xi$ is odd in the nontrivial case.[50–52,67,69,86–102]

Insulators with nontrivial $C_1$ or $\Xi$ exhibit spectral flow in the energy spectrum: on a lattice with boundaries, a set of protected edge states interpolates across the energy gap, such that the conduction and valence bands are spectrally connected.[49] For these insulators, spectral flow is also manifest in their single-particle entanglement spectra, where states close to eigenvalue 1 (0) form the entanglement analog of conduction (valence) bands.[48,54] Spectral flow is also known to exist in the $\mathcal{W}$-spectrum of these insulators, i.e., the Wannier trajectories interpolate across the full unit cell: $\vartheta \in [0,2\pi]$, where $\vartheta$ is the phase of the $\mathcal{W}$-eigenvalues; the symmetries that protect spectral flow are charge conservation (for the Chern insulator) and time-reversal symmetry (for the $\mathbb{Z}_2$ insulator).[57,67,86]

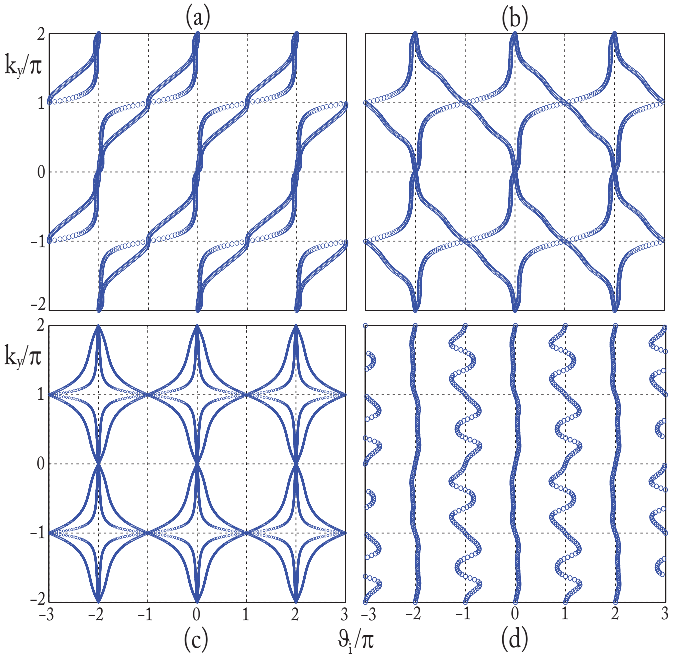

FIG. 1. Wannier center flows for four different phases. Each figure contains three unit cells in an effective 1D-lattice along $\hat{x}$; we track the real-space trajectories of Wannier centers (blue circles) in $\hat{x}$ as $k_y$ is varied through two adiabatic cycles. (a) An insulator with Chern number $C_1 = 2$ and zero relative winding ($W$); this is modelled by the Hamiltonian (27) with parameters $m = 3$ and $\delta = 2$. (b) An insulator with relative winding $W = 1$ and zero $C_1$; this is modelled by Eq. (27) with $m = 3$ and $\delta = 1$. (c) $W = 2$ and $C_1 = 0$; this is modelled by Eq. (31). (d) $W = 0$ and $C_1 = 0$; the phase has a nontrivial polarization, and is modelled by Eq. (24) with parameters $\alpha$ = -1.5, $\beta$ = 1.5, $\delta$ = -1.

It has been demonstrated in Ref. 48 that spectral flow, as protected only by $\mathcal{I}$ symmetry, does not exist in the physical energy and entanglement spectra; $\mathcal{I}$-symmetric topological insulators generically have protected mid-gap entanglement modes, without spectral flow. In this paper, we report that $\mathcal{I}$-protected spectral flow manifests only in the $\mathcal{W}$-spectrum, and is characterized by a relative winding number $W$; $W$ provides a $\mathbb{Z}$ classification of 2D $\mathcal{I}$-symmetric insulators. Two Wannier trajectories are said to wind relative to each other if they (i) intersect the *same* atomic site at a symmetric time $K_y$, then (ii) separate and intersect *adjacent* mid-bond sites half a period later $(K_y + \pi)$. $W$ is defined as the number of stable pairs of relatively-winding trajectories. For illustration, we plot the Wannier flows for the cases (i) $C_1 = 2$, $W = 0$ (Fig. 1-a), (ii) $W = 1$, $C_1 = 0$ (Fig. 1-b) and (iii) a TRS insulator with $W = 2$ and $\Xi = 0$ (Fig. 1-c). While these three nontrivial examples exhibit various forms of spectral flow, the absence of spectral flow does not imply a trivial insulator. A case in point is the 'weak' $\mathcal{I}$-symmetric topological insulator of Fig. 1-d, which may be thought of as a coupled array of 1D

$\mathcal{I}$-symmetric topological insulators; here, spectral flow is absent ($W = C_1 = 0$), yet the insulator has a nontrivial polarization in $\hat{x}$.

As exemplified in Tab. I, the mapping between $\mathcal{I}$ and $\mathcal{W}$-eigenvalues also applies to symmetric lines in the 2D BZ, e.g., $k_y = 0$ and $\pi$. For symmetric Wilson loops at constant $K_y = \{0, \pi\}$, let us define the number of +1, -1 and complex-conjugate-pair eigenvalues as $N_{(+1)}(K_y), N_{(\text{-}1)}(K_y)$ and $N_{(cc)}(K_y)$ respectively; these quantities constrain the possible Wannier trajectories that interpolate between $K_y = 0$ and $\pi$, and by implication they also constrain the possible topological invariants: $W$, $C_1$ and $\Xi$. These constraints are summarized in Tab. II, where we define $N_d$ as the maximum of two quantities:

$$\begin{aligned} N_d = \max \{ \; & N_{(\text{-}1)}(\pi) - N_{(\text{-}1)}(0) - N_{(cc)}(0), \\ & N_{(\text{-}1)}(0) - N_{(\text{-}1)}(\pi) - N_{(cc)}(\pi) \; \}. \end{aligned} \tag{2}$$

|  | $U(1)$ | TRS |
|---|---|---|
| $W > 0$ | $2W + \lvert C_1 \rvert = N_d$ | $W = \frac{1}{2} N_d$;<br>$\Xi = W \text{ mod } 2$ |
| $W = 0$ | $\lvert C_1 \rvert \geq N_d$;<br>$C_1 = N_{(\text{-}1)}(0) - N_{(\text{-}1)}(\pi)$ mod 2 | $\Xi = \frac{1}{2} \left( N_{(\text{-}1)}(0) - N_{(\text{-}1)}(\pi) \right)$ mod 2 |

TABLE II. Relations between relative winding $W \in \mathbb{Z}$, the Chern number $C_1 \in \mathbb{Z}$, the TR invariant $\Xi \in \mathbb{Z}_2$, and eigenvalues of the Wilson loop at symmetric momenta. Columns: $U(1)$ denotes a generic insulator with charge-conservation symmetry; TRS denotes a time-reversal symmetric insulator. $N_d$ is defined in Eq. (2).

In the remainder of the introduction, we extend our discussion of the 1D $\mathcal{I}$-symmetric insulator. What does it mean for a topological insulator to be nontrivial, and what role does inversion symmetry play? We define a nontrivial insulator by what it is not, up to gap- and symmetry-preserving transformations: an atomic insulator – a lattice of spatially-isolated atoms. How do we distinguish the $\mathcal{W}$-spectrum of a trivial insulator from one of a nontrivial insulator? In the atomic limit, all Bloch eigenfunctions are independent of crystal momentum, therefore the connection $C$ vanishes and $\mathcal{W}$ equals the identity in the occupied subspace. Having $\mathcal{W}$-eigenvalues that deviate from +1 is not a sufficient condition for nontriviality – by a gap- and symmetry-preserving transformation of the ground state, we may find that $\mathcal{W}$ is homotopically equivalent to the identity. A case in point is the 1D time-reversal symmetric (TRS) insulator, for which the $\mathcal{W}$-spectrum consists of Kramers degeneracies which may be tuned to any value, including +1.[57–59] However, suppose a subset of the $\mathcal{W}$-spectrum is fixed by symmetry to a special value other than +1 – our inability to transform the $\mathcal{W}$ to the identity indicates that the insulator is topologically distinct from the atomic insulator. In this paper we demonstrate that the discrete nature of the simplest point-group symmetry ($\mathcal{I}$) is reflected in a discrete $\mathcal{W}$-spectrum – a subset of $\mathcal{I}$-symmetric insulators have $\mathcal{W}$-eigenvalues that are fixed at -1, hence these insulators satisfy the criterion for nontriviality. In 1D, inversion $\mathcal{I}$ maps the spatial coordinate: $x \rightarrow \text{-}x$, where the inversion center ($x = 0$) is chosen to lie on an atomic site. In the momentum representation, $\mathcal{I}$ maps $k \rightarrow \text{-}k$, and an $\mathcal{I}$-symmetric insulator is characterized by the $\mathcal{I}$-eigenvalues of its occupied bands at symmetric momenta 0 and $\pi$. If the wavefunction at 0 and $\pi$ transform under different representations of $\mathcal{I}$, we find that a subset of the $\mathcal{W}$-spectrum is robustly quantized to -1. To quantify a change in the group representations between 0 and $\pi$, we look to the absolute difference in the number of same-symmetry bands between 0 and $\pi$: if there are $n_{(-)}(0)$ negative-$\mathcal{I}$ bands at 0 and $n_{(-)}(\pi)$ of them at $\pi$, we find that

$$N_{(\text{-}1)} = |n_{(-)}(0) - n_{(-)}(\pi)|, \tag{3}$$

where $N_{(\text{-}1)}$ is the number of symmetry-protected -1 $\mathcal{W}$-eigenvalues. In principle, $N_{(\text{-}1)}$ is detectable by holonomy: if we adiabatically transport an insulating ground state with $n_{occ}$ occupied bands around the 1D BZ, $N_{(\text{-}1)}$ of $n_{occ}$ electrons pick up Berry phases of $\pi$, which is detectable by interference. In practice, the coherent transport of electrons across the entire BZ is impeded by scattering from phonons, impurities and many-body effects. Despite these difficulties, Bloch oscillations and Wannier-Stark ladder states[103–107] have been observed in semiconductor superlattices[108] and with cold atoms in accelerated optical lattices.[109–112] These systems are the likeliest candidates to realize such an interference experiment.

While the Wilson-loop index $N_{(\text{-}1)}$ characterizes the bulk of a 1D $\mathcal{I}$-symmetric insulator, it is instructive to reformulate $N_{(\text{-}1)}$ from the perspective of the insulator's boundary modes. On a lattice with spatial boundaries, a variety of topological insulators may be classified through a stability analysis of their boundary modes.[59,113] For example, if one boundary mode is stable but two is not, we deduce that the classification is $\mathbb{Z}_2$. While 1D $\mathcal{I}$-symmetric insulators have no protected boundary modes in the physical energy spectrum, Turner *et al.* have demonstrated that these insulators manifest protected boundary modes in the entanglement spectrum – these modes localize at fictitious boundaries created by a spatial entanglement cut.[46,47] As demonstrated in Ref. 48 and 71, the number ($\chi \in \mathbb{Z}$) of stable modes at each entanglement boundary is equal to the absolute difference in the number of same-symmetry bands between 0 and $\pi$:

$$\chi = |n_{(-)}(0) - n_{(-)}(\pi)|. \tag{4}$$

Upon proving the identity (3), we identify $\chi = N_{(\text{-}1)}$, and thus establish a correspondence between the bulk of a 1D $\mathcal{I}$-symmetric insulator and its entanglement boundary.

Let us offer a third perspective through the geometric-phase theory of polarization, where the phases of the $\mathcal{W}$-eigenvalues represent spatial coordinates of the maximally-localized Wannier functions (WF), or just Wannier centers.[114,115] An eigenvalue of +1 implies the presence of a Wannier center at each atomic site in the periodic 1D lattice; -1 implies the presence of a Wannier center at each mid-bond site. In a study of $\mathcal{I}$-symmetric insulators with a single occupied band,[116] Kohn demonstrated that there are two classes of WF's:
(i) The WF is either symmetric or antisymmetric about the atomic site ($x = 0$). This occurs when (i-a) both Bloch waves with symmetric momenta $k = 0$ and $\pi$ are nodeless at $x = 0$, or (i-b) they both possess nodes at $x = 0$.
(ii) The WF is either symmetric or antisymmetric about the mid-bond site ($x = a/2$). This occurs when only one of the two symmetric-momentum Bloch waves has a node at $x = 0$.
Subsequently, Zak connected these observations to the modern theory of polarization, and showed that the Abelian $\mathcal{W}$ is quantized to +1 in case (i) and to -1 in case (ii).[62,63] Remarkably, (i) and (ii) are distinguished only by the group representations of the two Bloch waves at 0 and $\pi$. One aim of this paper is to extend this Abelian result to the non-Abelian $\mathcal{W}$, so that we may characterize $\mathcal{I}$-symmetry insulators with multiple occupied bands; many realistic materials defy a single-band description, due to interband degeneracies such as those enforced by time-reversal symmetry.[48,86]

The outline of this paper: in Sec. I, we introduce Brillouin-zone Wilson loops and explain their connections with polarization and holonomy. We analyze the 1D $\mathcal{I}$-symmetric insulator in Sec. II. Here, we (i) derive a mapping between $\mathcal{I}$ and $\mathcal{W}$ eigenvalues, and (ii) formulate the topological index $N_{(\text{-}1)}$ which provides us a $\mathbb{Z}$ classification. We analyze the 2D $\mathcal{I}$-symmetric insulator in Sec. III. Here, we (a) describe how the $\mathcal{W}$-spectrum is constrained by $\mathcal{I}$ and TRS, (b) identify a relative winding number $W$ which characterizes $\mathcal{I}$-protected spectral flow, and (c) elucidate relations between various topological invariants $(W, C_1, \Xi)$ and the $\mathcal{W}$-eigenvalues at symmetric lines in the 2D BZ. We conclude in Sec. IV.

## I. INTRODUCTION TO BRILLOUIN-ZONE WILSON LOOPS

The Brillouin-zone Wilson loop is pedagogically introduced; we describe its role in holonomy (Sec. I A) and in the geometric-phase theory of polarization (Sec. I B). In Sec. I C, we explain the construction of a coarse-grained Wilson loop from a tight-binding Hamiltonian, for the purpose of numerically computing topological invariants.

The Hamiltonian for a single particle is

$$H = \frac{p^2}{2m} + V(r). \tag{5}$$

If $V(r) = V(r+R)$ for any lattice vector $R$, this Hamiltonian is symmetric under discrete translations. Consequently, $H$ decouples into representations labelled by the crystal momentum $k$; an eigenstate in the $n$'th band may be written in Bloch form: $\psi^n_k(r) = e^{ikr}\, u^n_k(r)$, where $u^n_k(r) = u^n_k(r+R)$ is a function that is periodic in lattice translations, and also satisfies:

$$\left[ \frac{(p+\hbar k)^2}{2m} + V(r) - \varepsilon^n_k \right] u^n_k(r) = 0. \tag{6}$$

Each eigenstate has a corresponding projection $\mathcal{P}^n_k(r,r') = u^n_k(r)\, u^{n*}_k(r')$; the many-body ground-state is a single Slater determinant of all single-particle eigenstates with energies less than the Fermi energy. The topological properties of an insulator are invariant under transformations of the Hamiltonian that preserve both the energy gap and the symmetry that stabilizes the topological phase. We perform one such transformation by setting the energies of all eigenstates $u^n_k$ below (above) the Fermi energy equal to $\varepsilon_{\text{-}}$ $(\varepsilon_+)$. Denoting the projection onto the $n_{occ}$ occupied bands as $\mathcal{P}^{\text{occ}}_k = \sum_{i=1}^{n_{occ}} \mathcal{P}^n_k$, we express the resultant flat-band Hamiltonian as

$$\mathcal{H}_{\text{F}}(k) = (\varepsilon_{\text{-}} - \varepsilon_+)\, \mathcal{P}^{\text{occ}}_k + \varepsilon_+ I. \tag{7}$$

Eq. (7) has a gauge redundancy which is not apparent in (6) – the ground-state projection $\mathcal{P}^{\text{occ}}_k$ is invariant under a local $U(n_{occ})$ gauge transformation in the $n_{occ}$-dimensional subspace of occupied bands: $u^n_k \rightarrow u^m_k M^{mn}_k$ with $m, n = 1 \dots n_{occ}$ and $M^{\text{-}1}_k = M^\dagger_k$.

### A. Wilson Loop as arising from Holonomy

The adiabatic transport of a ground state at initial momentum $k^{(i)}$ to a final momentum $k$ involves a unitary rotation of the basis vectors $u^n_k$ in the subspace of occupied bands. This $U(n_{occ})$ rotation is affected by a Wilson-line matrix $\mathcal{W}_{k \leftarrow k^{(i)}}$ that maps the subspace of occupied bands at $k^{(i)}$ to the subspace of occupied bands at $k$. $\mathcal{W}$ is known to satisfy a parallel transport equation

$$\tfrac{\partial}{\partial k_\mu}\, \mathcal{W}_{k \leftarrow k^{(i)}} = \text{-}\, C_k(k_\mu)\, \mathcal{W}_{k \leftarrow k^{(i)}}, \tag{8}$$

with the connection $C$ defined as

$$C^{mn}_k(k_\mu) = \int d^d r\; u^m_k(r)^*\, \tfrac{\partial}{\partial k_\mu}\, u^n_k(r). \tag{9}$$

Here, $k_\mu \in \{k_1, \dots, k_d\}$ denote momenta components in a $d$-dimensional BZ. Eq. (8) is pedagogically derived in

App. A. This differential equation has the path-ordered solution

$$\mathcal{W}_{k\leftarrow k^{(i)}}(\mathcal{L}) = \mathrm{T}\,\exp\big[\,\text{-}\int_{\mathcal{L}} C_q(q_\mu)\;dq_\mu\,\big] \tag{10}$$

for a path $\mathcal{L}$ that connects momenta $k$ and $k^{(i)}$. (10) is a matrix representation of a holonomy, *i.e.*, a parallel transport map.[64] If $k = k^{(i)}$ modulo a reciprocal vector, $\mathcal{L}$ forms a closed circuit in the BZ and we denote the resultant $U(n_{occ})$ Wilson loop as $\mathcal{W}$; *cf.* (1).

### B. Wilson Loops in the Geometric-Phase Theory of Polarization

Let us derive a well-known relation between $\mathcal{W}$ and the polarization of a 1D insulator. For a group of $n_{occ}$ occupied bands, the delocalized Bloch waves $\psi^m_k$ form an orthonormal basis in the occupied Hilbert space; $m = 1, 2, \ldots, n_{occ}$. Assuming a periodic gauge ($\psi^m_k = \psi^m_{k+2\pi}$), we formulate the theory of polarization in an alternative basis of localized Wannier functions (WF):

$$\Psi^{(j)}(x-R) = \int \frac{dk}{2\pi}\, e^{-ikR} \sum_{n=1}^{n_{occ}} O(k)_{jn}\; \psi^n_k(x). \tag{11}$$

Each WF $\Psi^{(j)}(x-R)$ is labelled by the unit cell $R \in \mathbb{Z}$ and an index $j = 1, 2, \ldots n_{occ}$. If $n_{occ} = 1$, $O(k)$ is a momentum-dependent phase; if $n_{occ} > 1$, $O(k)$ is a $U(n_{occ})$ matrix that affects rotations in the subspace of degenerate bands. The gauge freedom in $O(k)$ is fixed, up to trivial $U(1)$ phase windings, by requiring that the WF's are maximally localized.[115] Equivalently, we require that the WF's are eigenfunctions of the projected position operator $\mathcal{P}^{\text{occ}}\,\hat{x}\,\mathcal{P}^{\text{occ}}$:[114]

$$\big(\,\mathcal{P}^{\text{occ}}\,\hat{x}\,\mathcal{P}^{\text{occ}} - \tfrac{1}{2\pi}\,\vartheta^{(j)} - R\,\big)\;\Psi^{(j)}(x-R) = 0. \tag{12}$$

Here, $\mathcal{P}^{\text{occ}}$ projects to the occupied subspace, and all lengths are in units of the lattice constant. We show in App. C that the spectrum $\{\vartheta^{(j)}\}$ coincide with the phases of the $\mathcal{W}$-spectrum. Through (12) we map the electron density to classical point charges at the positions $\{\vartheta^{(j)}/2\pi + R\}$; we call these positions the Wannier centers. If $\vartheta = 0$, there exists a Wannier center at each atomic site; if $\vartheta = \pi$, there exists a Wannier center in the middle of two adjacent atomic sites – we call this the mid-bond site. For an atomic insulator, $\mathcal{W}$ equals the identity in the occupied subspace; this implies that all the Wannier centers sit at the atomic sites.

### C. The Tight-Binding Wilson Loop

As defined in (1), the continuum Wilson loop $\mathcal{W}$ is expensive to compute numerically. In this Section, we introduce the tight-binding Wilson loop $\mathcal{W}_A$, which is computable with relative ease. In the tight-binding approximation, we restrict our attention to nearly-degenerate orbitals which diagonalize the atomic Hamiltonian. The Hamiltonian of (5) reduces to the variational form

$$H = \sum_k c^\dagger_{k\alpha}\;[h(k)]_{\alpha\beta}\;c_{k\beta} \tag{13}$$

with orbital indices $\alpha, \beta$; $[h(k)]_{\alpha\beta}$ are the matrix elements of (5) in the Bloch basis of Löwdin orbitals.[117–119] In (13) and the rest of the paper, we sum over repeated indices. Let us denote the $j$-th normal mode operator as $\gamma^\dagger_{jk} = [U^j_k]_\beta\, c^\dagger_{k\beta}$; in bra-ket notation, the corresponding projection is $\mathcal{P}^j_k = |U^j_k\rangle\langle U^j_k| = \gamma^\dagger_{jk}|0\rangle\langle 0|\gamma_{jk}$. We define the tight-binding connection $A$ as

$$A^{mn}_k(k_\mu) = \big\langle U^m_k\big|\,\tfrac{\partial}{\partial k_\mu}\,\big|U^n_k\big\rangle, \tag{14}$$

The tight-binding Wilson loop $\mathcal{W}_A$ is defined as the path-ordered exponential of the tight-binding connection $A$:

$$\mathcal{W}_A = \mathrm{T}\,\exp\big[\,\text{-}\int dq_\mu\; A_q(q_\mu)\,\big]. \tag{15}$$

A discretized expression of $\mathcal{W}_A$ is obtained by dividing a BZ loop $\mathcal{L}$ into infinitesimally-separated momenta: $\{k^{(0)}{+}G, k^{(N)}, k^{(N\text{-}1)} \ldots k^{(2)}, k^{(1)}, k^{(0)}\}$ with $N \gg 1$. Defining $\mathcal{P}^{\text{occ}}_k = \sum_{j=1}^{n_{occ}} \mathcal{P}^j_k$ as the projection to the occupied bands, $\mathcal{W}_A$ may be expressed as a path-ordered product of projections, sandwiched by tight-binding eigenfunctions at the base and end points:

$$[\mathcal{W}_A(\mathcal{L})]^{mn} = \big\langle U^m_{k^{(0)}+G}\big|\;\mathrm{T}\prod_{\alpha=1}^{N} \mathcal{P}^{\text{occ}}_{k_\alpha}\;\big|U^n_{k^{(0)}}\big\rangle. \tag{16}$$

The product of projections are path-ordered along $\mathcal{L}$, with the earlier-time momenta positioned to the right. In App. D, we show that $A$ is related to the continuum connection $C$, as defined in (9), through

$$C_k(k_\mu) = A_k(k_\mu) - i\,[\hat{r}_\mu]_k + i\,\bar{R}_\mu, \tag{17}$$

where $\hat{r}_\mu$ is the position operator in the basis of occupied bands and $\bar{R}_\mu$ is the average atomic displacement in the direction $\mu$. Since $A$ and $C$ differ by $[\hat{r}_\mu]_k - \bar{R}_\mu$, we expect that the tight-binding Wilson loop (15) and the continuum Wilson loop (1) generically have different eigenspectra. However, we show in App. E that both Wilson loops are identically constrained by inversion symmetry, and consequently their spectra are nearly identical. In particular, the topological index $N_{(\text{-}1)}$, as defined in the Introduction, may be extracted from either Wilson loop. To simplify the presentation in the next Section, we speak only of the tight-binding Wilson loop, which we henceforth denote as $\mathcal{W}$.

## II. WILSON-LOOP CHARACTERIZATION OF THE 1D INVERSION-SYMMETRIC INSULATOR

We highlight distinctive features of the $\mathcal{I}$-symmetric Wilson loop (Sec. II A), and present a mapping between the $\mathcal{W}$-eigenvalues and the $\mathcal{I}$ eigenvalues of the ground state (Sec. II B). In Sec. II C, we formulate the topological index $N_{(\text{-}1)} \in \mathbb{Z}$ that classifies $\mathcal{I}$-symmetric insulators. In addition, we relate $N_{(\text{-}1)}$ to a well-known $\mathbb{Z}_2$ index that distinguishes the electric responses of these insulators.

### A. Constraints on the Wilson Loop due to Inversion Symmetry

As shown in App. D, a tight-binding Hamiltonian with $\mathcal{I}$ symmetry satisfies $\wp\, h(k)\, \wp = h(\text{-}k)$, where $\wp$ is the overlap matrix:

$$\wp_{\alpha\beta} = \int dx\; \phi^*_\alpha(x)\, \phi_\beta(\text{-}x); \tag{18}$$

$\alpha, \beta$ are orbital indices and $\{\phi_\alpha\}$ are eigenfunctions of the atomic Hamiltonian. This implies that the occupied eigenstates $U^m_k$ at $\pm k$ are related through inversion by a $U(n_{occ})$ 'sewing matrix' $B_k$:

$$[U^m_{\text{-}k}]_\alpha = \sum_{n=1}^{n_{occ}} \sum_\beta B^{mn*}_k\, \wp_{\alpha\beta}\, [U^n_k]_\beta. \tag{19}$$

Here, $m, n$ are indices that label the occupied bands. Due to the $U(n_{occ})$ gauge freedom in the occupied subspace, the sewing matrix $B_k$ is gauge-variant. In deriving the gauge-invariant $W$-eigenspectrum, we will employ a gauge in which $U^n_{k^{\text{inv}}}$ are eigenstates of $\mathcal{I}$ at inversion-invariant momenta $k^{\text{inv}}$; $B_{k^{\text{inv}}}$ is then a diagonal matrix with diagonal elements equal to the $\mathcal{I}$ eigenvalues of $U^n_{k^{\text{inv}}}$.

Given $B_k$ and its analytic properties, we derive the following properties for an $\mathcal{I}$-symmetric Wilson loop:

(i) $\mathcal{W}$ is unitarily equivalent to its Hermitian adjoint, *i.e.*, the *set* of $\mathcal{W}$-eigenvalues is equal to its complex conjugate:

$$\big\{\exp i\vartheta\big\} = \big\{\exp \text{-}i\vartheta\big\}. \tag{20}$$

This implies that the eigenvalues of $\mathcal{W}$ are constrained to $\pm 1$ or otherwise form complex-conjugate pairs. Equivalently stated, the Wannier centers localize (i) at the atomic site (+1) or (ii) at the mid-bond site (-1) or (iii) form pairs that localize equidistantly on opposite sides of each atomic site ($\lambda\lambda^*$). In all three cases, the spatial configuration of Wannier centers is invariant under a spatial inversion $x \to \text{-}x$.

(ii) Let $\mathcal{L}$ be a BZ loop beginning at $k^{(0)} = \text{-}\pi$ and ending at $\pi$. The Wilson loop along $\mathcal{L}$ may be decomposed into two Wilson lines that each connect two symmetric momenta: $\mathcal{W}(\mathcal{L}) = \mathcal{W}_{\pi\leftarrow 0}\, \mathcal{W}_{0\leftarrow\text{-}\pi}$. Up to a change in orientation, $\mathcal{W}_{\pi\leftarrow 0}$ is mapped to $\mathcal{W}_{0\leftarrow\text{-}\pi}$ by an inversion $k \to \text{-}k$. It follows from the sewing condition (19) that

$$\mathcal{W}(\mathcal{L}) = B_\pi\, [\mathcal{W}_{0\leftarrow\text{-}\pi}]^\dagger\, B_0\, \mathcal{W}_{0\leftarrow\text{-}\pi}. \tag{21}$$

The symmetry constraints (19),(20) and (21) are derived in App. E; these results are applied in the next Section, where we derive a mapping between $\mathcal{W}$-eigenvalues and the $\mathcal{I}$ eigenvalues of the occupied bands.

### B. 1D: Mapping between Wilson-loop and Inversion Eigenvalues

For a subset of $\mathcal{I}$-symmetric ground states, their $\mathcal{W}$-spectra comprise only $\pm 1$ eigenvalues. This occurs if the $\mathcal{I}$ eigenvalues of occupied bands at either $k = 0$ or $\pi$ are the same; then the $\mathcal{W}$-spectrum comprises the diagonal elements of the product of sewing matrices: $B_0\, B_\pi$.
*Proof:* If at $k = 0$, the occupied bands have $\mathcal{I}$ eigenvalue $\bar{\xi}$, i.e., the sewing matrix $B_0 = \bar{\xi}\, I$, then from (21) we deduce that $\mathcal{W} = B_0\, B_\pi$. If instead $B_\pi = \bar{\xi}\, I$, then $\mathcal{W}$ is equivalent to $B_0\, B_\pi$ by a unitary transformation.

Let us define a quantity $n_s$ that equals zero for the above subset of ground states; $n_s > 0$ if the occupied bands have nonidentical $\mathcal{I}$ eigenvalues at *both* 0 and $\pi$.
*Definition:* For the occupied bands of an insulating phase, let us define the number of positive and negative $\mathcal{I}$ eigenvalues, at $k^{\text{inv}} = \{0, \pi\}$, by $n_{(+)}(k^{\text{inv}})$ and $n_{(-)}(k^{\text{inv}})$. Given this set of four numbers $\{\, n_{(+)}(0), n_{(-)}(0), n_{(+)}(\pi), n_{(-)}(\pi)\, \}$, we identify the smallest of the four and label it as $n_s$, *i.e.*, $n_s$ is the number of the Fewest Bands of One Symmetry among both symmetric momentum $k^{\text{inv}}$; we call these bands the FBOS. We label the momentum where FBOS lies as $k_s$ and the $\mathcal{I}$ eigenvalue of FBOS as $\xi_s$. Let us identify the FBOS for the following examples.
(a) Consider a two-band insulator with $\mathcal{I}$ eigenvalues $(++)$ at $k = 0$ and $(+-)$ at $k = \pi$. The FBOS are the negative-$\mathcal{I}$ bands at $k_s = 0$. None exists, so $n_s = 0$.
(b) Suppose we had a four-band insulator with $\mathcal{I}$ eigenvalues $(++--)$ at $k = 0$ and $(+++-)$ at $k = \pi$, the FBOS is the single negative-$\mathcal{I}$ band at $k_s = \pi$, so $\xi_s = \text{-}1$ and $n_s = 1$.
(c) If a subset of the four numbers $\{n_{(\pm)}(k^{\text{inv}})\}$ are equally small, we may denote any number in this subset as $n_s$. In a two-band example, we may encounter $n_{(+)}(0) = n_{(-)}(0) = n_{(+)}(\pi) = n_{(-)}(\pi) = 1$. Then, one may label any of the four possibilities as the FBOS.

*Mapping:* Given an inversion-symmetric insulator that is characterized by the quantities $\{\, n_{(\pm)}(k^{\text{inv}}), n_s, k_s, \xi_s\, \}$, its Wilson-loop eigenspectrum consists of:
(i) $(n_{(+)}(k_s + \pi) - n_s)$ number of $\text{-}\xi_s$ eigenvalues,
(ii) $(n_{(-)}(k_s + \pi) - n_s)$ number of $\xi_s$ eigenvalues, and
(iii) $n_s$ pairs of complex-conjugate eigenvalues.

In the above examples, the $\mathcal{W}$-spectrum of insulator (a) comprises one +1 and one -1 eigenvalue; for insulator (b), there are one +1 eigenvalue, one -1 eigenvalue, and one complex-conjugate pair; insulator (c) has one complex-conjugate pair only. The proof of this mapping is detailed in App. G. The interested reader also may refer to App. F, where we undertake the case studies of the one- and two-band $\mathcal{W}$'s; these case studies offer an intuitive understanding of the above mapping, and also provide an alternate derivation that is specific to one and two occupied bands. For an insulator with one, two and four occupied bands, we tabulate the possible mappings in Tab. III, IV and I respectively.

Let us define a $\mathbb{Z}$ index, $N_{(-1)}$, as the number of -1 eigenvalues in the $\mathcal{W}$-spectrum. It is possible that one or more pairs of complex-conjugate eigenvalues are accidentally degenerate at -1; we exclude them from the definition of $N_{(-1)}$. Through the above mapping, we deduce that $N_{(-1)}$ is the absolute difference in the number of same-symmetry bands between 0 and $\pi$, and quantifies the change in the group representation; *cf.* Eq. (3). In the following Section, we argue that a nonzero $N_{(-1)}$ is an indication of topological nontriviality.

| $\mathcal{I}$ eigenvalues | $\mathcal{W}$-spectrum |
|---|---|
| $\{(+)\,(+)\}$ | $[+]$ |
| $\{(+)\,(-)\}$ | $[-]$ |

TABLE III. For an insulator with one occupied band, we tabulate the $\mathcal{I}$ eigenvalues of the occupied band at symmetric momenta $\{0,\pi\}$ and the corresponding $\mathcal{W}$-spectrum. $+$ $(-)$ refers to an eigenvalue of +1 (-1). $\{(+)\,(-)\}$ may refer to either (i) a positive-$\mathcal{I}$ band at $k=0$, with a negative-$\mathcal{I}$ band at $\pi$, or (ii) a negative-$\mathcal{I}$ band at 0, with a positive-$\mathcal{I}$ band at $\pi$. If two sets of $\mathcal{I}$ eigenvalues (from two distinct insulators) are related by a global change in sign, they are mapped to the same $\mathcal{W}$ eigenvalue. For example, both $\{(+)\,(+)\}$ and $\{(-)\,(-)\}$ are mapped to $\mathcal{W}=$ +1.

| | $\mathcal{I}$ eigenvalues | $\mathcal{W}$-spectrum |
|---|---|---|
| (i) | $\{(++)\,(++)\}$ | $[++]$ |
| (ii) | $\{(++)\,(+-)\}$ | $[+-]$ |
| (iii) | $\{(++)\,(--)\}$ | $[--]$ |
| (iv) | $\{(+-)\,(+-)\}$ | $[\lambda\lambda^*]$ |

TABLE IV. For an insulator with two occupied bands, we tabulate the $\mathcal{I}$ eigenvalues of the occupied bands at symmetric momenta $\{0,\pi\}$ and the corresponding $\mathcal{W}$-spectrum. We collect the $\mathcal{I}$ eigenvalues $\xi_i$ at each symmetric momenta into $(\xi_1\ \xi_2)$.

## C. 1D: Topological Invariants from the Wilson Loop

### 1. $\mathbb{Z}$ Index: Number of Robust -1 Wilson-Loop Eigenvalues

A nonzero $N_{(-1)}$ index obstructs $\mathcal{W}$ from being tuned to the identity – the atomic limit; this is a sufficient condition for nontriviality. While complex-conjugate $\mathcal{W}$-eigenvalues $[\lambda,\lambda^*]$ also deviate from the atomic value of +1, they are not a sufficient condition for nontriviality. The exact value of $\lambda$ is not fixed by symmetry; this arbitrariness reflects the range in this equivalence class, *i.e.*, it is possible to tune the Hamiltonian and sweep the interval of allowed $\lambda$ while preserving both gap and symmetry. In particular, we can always tune the complex-conjugate eigenvalues to the trivial limit of [+1, +1]. It is possible that pairs of complex-conjugate eigenvalues are accidentally degenerate at -1. Unlike the $N_{(-1)}$ values of -1, these extra degeneracies are not protected by $\mathcal{I}$ – they generically destabilize under a soft deformation of the ground-state, hence they do not indicate a nontrivial phase. Hence, symmetry dictates that $N_{(-1)}$ is the *minimum* number of -1 eigenvalues; there are two implications:

(i) Suppose we begin with a nontrivial insulator with $N_{(-1)} > 0$, and we would like to transform it to an atomic insulator while preserving $\mathcal{I}$ symmetry. The energy gap must close a minimum of $N_{(-1)}$ times at a symmetric momentum, before the atomic limit ($N_{(-1)}=0$) is reached. In each gap-closing event, a pair of opposite-sign $\mathcal{I}$-eigenvalues are inverted between occupied and unoccupied bands, thus reducing $N_{(-1)}$ by one.

(ii) As formulated in the entanglement spectrum, the criterion for nontriviality is the existence of protected boundary modes in the gap of the single-particle entanglement spectrum. For an $\mathcal{I}$-symmetric insulator, the number ($\chi \in \mathbb{Z}$) of stable modes at each entanglement boundary is equal to the absolute difference in the number of same-symmetry bands between 0 and $\pi$; *cf.* (4).[48,71] Thus, we identify $\chi$ with the $\mathcal{W}$-index $N_{(-1)}$, and show that the two formulations of nontriviality are equivalent.

### 2. $\mathbb{Z}_2$ Polarization Index: Determinant of $\mathcal{W}$

The determinant of $\mathcal{W}$, which we define as $\mathcal{D}$, is the exponentiated polarization of the 1D insulator. Since all $\mathcal{W}$-eigenvalues are either $\pm 1$ or form complex-conjugate pairs, $\mathcal{D}$ is quantized to $\pm 1$ - the classification of the electric response is $\mathbb{Z}_2$, as is recognized in works such as Ref. 48 and 63. Moreover, $\mathcal{D}$ is only determined by the number of -1 eigenvalues: $\mathcal{D} = (\text{-}1)^{N_{(-1)}}$. Let us relate $\mathcal{D}$ to the $\mathcal{I}$ eigenvalues of the ground state. From (3) we have that

$$\mathcal{D} = (\text{-}1)^{|n_{(-)}(0)-n_{(-)}(\pi)|} = \prod_{k^{\text{inv}}=0,\pi} \prod_{m=1}^{n_{occ}} \xi^m_{k^{\text{inv}}}, \qquad (22)$$

where $\xi^m_{k^{\text{inv}}}$ is the $\mathcal{I}$ eigenvalue of the $m$'th band at symmetric momentum $k^{\text{inv}}$. This concludes our discussion for 1D.

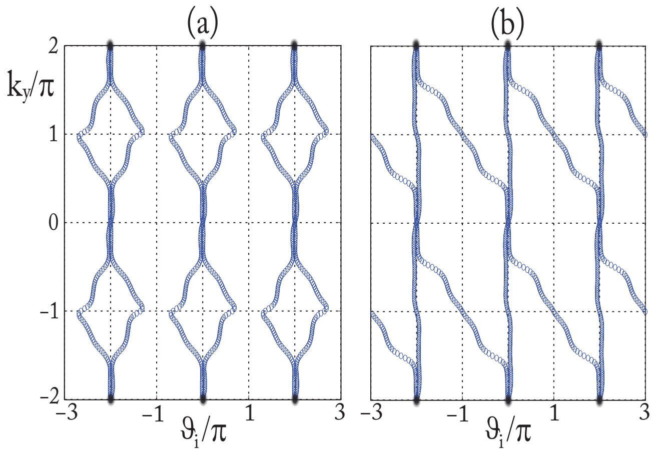

FIG. 2. The Wannier center flows for a 2D insulator with $\mathcal{I}$ symmetry. Each figure contains three unit cells in an effective 1D-lattice along $\hat{x}$; the positions of the atomic sites are indicated by black dots. The ground state contains two occupied bands, hence there are two Wannier centers in each unit cell. (a) This phase is realized in the model Hamiltonian (24), with parameters $\alpha =$ -1.5, $\beta = 1.5$ and $\delta = 1$. Upon $k_y \rightarrow k_y + 2\pi$, the pair of Wannier centers in each unit cell exchange positions. There is no net transfer of charge between unit cells, hence $C_1 = 0$. (b) This phase is realized in the same model with $\alpha =$ -1.5 and $\beta = 0$. Upon $k_y \rightarrow k_y + 2\pi$, *one* Wannier center adiabatically flows to its neighboring unit cell on the left. This represents a quantized Hall current, hence $C_1 =$ -1.

## III. WILSON-LOOP CHARACTERIZATION OF THE 2D INVERSION-SYMMETRIC INSULATOR

The Wilson loop $\mathcal{W}$ is known to encode the first Chern class $C_1$; we present a summary of this relation in Sec. III A. In Sec. III B, we impose $\mathcal{I}$ symmetry and investigate how the symmetry constrains $\mathcal{W}$ and the allowed Chern numbers. $\mathcal{W}$ is further constrained if the insulator is also time-reversal symmetric (TRS) – this is explored in Sec. III C. In Sec. III D, we introduce a relative winding number $W$ that characterizes insulators with $\mathcal{I}$-protected spectral flow. In addition, we derive relations between $W$, $C_1$, the time-reversal invariant $\Xi$, and Wilson-loop eigenvalues at symmetric lines in the 2D BZ.

### A. Wilson Loops and the First Chern Class

A well-known relation exists between Wilson loops and the integer quantum Hall effect. Let us apply an electric field along $\hat{y}$, which adiabatically translates all single-particle states in the parameter space $k_y$. To probe for a quantum Hall response, we study the $k_y$-evolution of the ground-state polarization (in $\hat{x}$) – we are interested in Brillouin-zone $\mathcal{W}$'s at constant $k_y$: $\mathcal{W}_{k_y} = \mathrm{T}\exp\left(\text{-}\int dk_x\, C_k(k_x)\right)$. Let us denote the $n_{occ}$ eigenvalues of $\mathcal{W}_{k_y}$ by the set $\{\exp(i\vartheta^m_{k_y})\}$. The geometric phase $\vartheta^m_{k_y}/2\pi$ represents the center of a hybrid Wannier function (WF), which extends in $\hat{y}$ in the manner of a 1D Bloch wave, but localizes in $\hat{x}$ as a 1D WF; we refer to these phases as the Wannier centers.[72] The derivative of the geometric phase, $\dot{\vartheta}^m_{k_y} \equiv d\,\vartheta^m/d\,k_y$, is interpreted as the real-space velocity (in $\hat{x}$) of the $m$'th Wannier center at time $k_y$. By integrating the velocities of all Wannier centers over a period $2\pi$, we obtain the net quantum Hall current. Thus, we identify the first Chern class as the center-of-mass winding:

$$C_1 = \sum_{m=1}^{n_{\mathrm{occ}}} \int \dot{\vartheta}^m_{k_y}\, \frac{dk_y}{2\pi}. \tag{23}$$

As we have shown in Sec. I B, polarization is directly related to the continuum Wilson loop, which is defined in (1). However, the winding number in the tight-binding Wilson loop, as defined in Sec. I C, is identical to that in the continuum Wilson loop. This follows because their connections differ by an operator that is periodic in $k_y$ (*cf.* Eq. (17) ). For the purpose of computing Chern numbers, both Wilson loops give identical results.

For illustration, we consider the 4-band model

$$\begin{aligned} h(k) &= \tfrac{1}{2}\,\Gamma_{13} + \tfrac{\alpha}{2}\,(\cos k_x + \cos k_y)\,(\Gamma_{30} + \Gamma_{03}) \\ &+ (\Gamma_{12} + \Gamma_{31})\,\sin k_x + (\Gamma_{21} + \Gamma_{32})\,\sin k_y - \Gamma_{03} \\ &+ \tfrac{\beta}{2}\,(\cos k_x)\,(\cos k_y - \delta)\,(\Gamma_{03} - \Gamma_{30}), \end{aligned} \tag{24}$$

where $h(k)$ is a matrix in the tight-binding basis; *cf.* (13). $\Gamma_{ij}$ are defined as $\sigma_i \otimes \tau_j$; $\sigma_0$ ($\tau_0$) is the identity in spin (orbital) space; $\sigma_{i=1,2,3}$ ($\tau_{i=1,2,3}$) are Pauli matrices in spin (orbital) space. The Hamiltonian possesses an $\mathcal{I}$ symmetry: $\Gamma_{03}\, h(k)\, \Gamma_{03} = h(\text{-}k)$. The Fermi energy is chosen so that there are two occupied bands in the ground state. We tabulate the $\mathcal{I}$ and $\mathcal{W}$-eigenvalues for various choices of the parameters ($\alpha, \beta$ and $\delta$) in Tab. V. In Fig. 2-a we plot the $\mathcal{W}_{k_y}$-spectrum for a trivial insulator ($\alpha =$ -1.5$, \beta = 1.5, \delta = 1$); Fig. 2-b corresponds to a nontrivial insulator with $C_1 =$ -1 ($\alpha =$ -1.5$, \beta = 0, \delta = 0$).

| Parameters | | | $\mathcal{I}$ eigenvalues | | | | $\mathcal{W}_{K_y}$ eigenvalues | |
|---|---|---|---|---|---|---|---|---|
| $\alpha$ | $\beta$ | $\delta$ | $(0,0)$ | $(\pi,0)$ | $(0,\pi)$ | $(\pi,\pi)$ | $K_y = 0$ | $K_y = \pi$ |
| -1.5 | 0 | 0 | $(++)$ | $(++)$ | $(++)$ | $(+-)$ | $[++]$ | $[+-]$ |
| -1.5 | 1.5 | 1 | $(++)$ | $(++)$ | $(+-)$ | $(+-)$ | $[++]$ | $[\lambda\lambda^*]$ |
| -1.5 | 1.5 | -1 | $(++)$ | $(+-)$ | $(++)$ | $(+-)$ | $[+-]$ | $[+-]$ |

TABLE V. The $\mathcal{I}$ and $\mathcal{W}_{K_y}$ eigenvalues of the ground state of Hamiltonian (24), for various parameters.

### B. The Inversion-Symmetric Wilson Loop and the Integer Quantum Hall Effect

Let us investigate the spectrum of the $\mathcal{I}$-symmetric $\mathcal{W}_{k_y}$. As derived in App. H, we find that $\mathcal{W}_{k_y}$ is equivalent to the Hermitian adjoint of $\mathcal{W}_{\text{-}k_y}$ by a unitary transformation, *i.e.*, the *sets* of $\mathcal{W}$-eigenvalues at $\pm k_y$ are equal up to complex conjugation:

$$\big\{\exp i\vartheta_{k_y}\big\} = \big\{\exp\text{-}i\vartheta_{\text{-}k_y}\big\}, \tag{25}$$

as may be verified in Fig. 2. At $K_y \in \{0,\pi\}$, the 1D line of states behaves like a 1D $\mathcal{I}$-symmetric insulator in two respects: (i) the eigenvalues of $\mathcal{W}_{K_y}$ are constrained to $\pm 1$ or otherwise form complex-conjugate pairs. (ii) In 1D, the $\mathcal{I}$ eigenvalues at $k=0$ and $\pi$ are related to $\mathcal{W}$-eigenvalues through the mapping of Sec. II B; in 2D, the $\mathcal{I}$ eigenvalues at momenta $(0,K_y)$ and $(\pi,K_y)$ are related to the eigenvalues of $\mathcal{W}_{K_y}$ through the same mapping.

Let us define the number of robust -1 eigenvalues in the spectra of $\mathcal{W}_0$ and $\mathcal{W}_\pi$ as $N_{(\text{-}1)}(0)$ and $N_{(\text{-}1)}(\pi)$ respectively. During the adiabatic evolution, $N_{(\text{-}1)}(K_y)$ is the number of Wannier centers that localize at each mid-bond site at time $K_y$. A difference in the indices $N_{(\text{-}1)}(0)$ and $N_{(\text{-}1)}(\pi)$ implies a net Hall current; moreover, the parity of the Chern number is determined through

$$N_{(\text{-}1)}(0) - N_{(\text{-}1)}(\pi) = C_1 \mod 2. \tag{26}$$

The two parities of $C_1$ correspond to the following situations:
(i) Suppose the parities of $N_{(\text{-}1)}(K_y)$ differ. Between $K_y=0$ and $\pi$, an *odd* number of Wannier centers must interpolate between the mid-bond sites ($\mathcal{W}$-eigenvalue of -1) and the non-mid-bond sites, which include (a) the atomic sites (+1) (see Fig. 2-b), and (b) the complex-conjugate sites ($\lambda\,\lambda^*$). The net translation of Wannier centers in the interval $k_y \in [0,\pi]$ is *half* an odd integer. It follows from (23) and (25) that $C_1$ is odd.
(ii) An analogous argument emerges when the parities of $N_{(\text{-}1)}(K_y)$ are equal. Now an *even* number of Wannier centers must interpolate between the mid-bond sites (at time $K_y=0$) and the non-mid-bond sites (at time $K_y=\pi$). One possible scenario is illustrated in Fig. (2-a). The conclusion is that $C_1$ is even.
It follows from Eq. (26), (3) and (22) that the product of all $\mathcal{I}$ eigenvalues (over all occupied bands at every symmetric momenta) has the same parity as $C_1$.

### C. The Inversion- and Time-Reversal-Symmetric Wilson Loop

Our aim is to highlight distinctive features of Wilson loops with both $\mathcal{I}$ and time-reversal symmetries; we illustrate these features with a four-band model Hamiltonian:

$$\begin{aligned} h(k) = {} & (2-m-\cos k_x-\cos k_y)\,\Gamma_{03} + \delta\,\sin k_y\,\Gamma_{12} \\ & +\,\sin k_x\,(\Gamma_{31}+\Gamma_{11}) +\,\sin k_y\,(\Gamma_{21}+\Gamma_{02}), \end{aligned} \tag{27}$$

with matrices $\Gamma_{ij}$ defined as $\sigma_i \otimes \tau_j$; $\sigma_0$ ($\tau_0$) is the identity in spin (orbital) space; $\sigma_{i=1,2,3}$ ($\tau_{i=1,2,3}$) are Pauli matrices in spin (orbital) space. The Hamiltonian is $\mathcal{I}$-symmetric: $\Gamma_{03}\,h(k)\,\Gamma_{03} = h(\text{-}k)$. The Fermi energy is chosen so that there are two occupied bands in the ground state. We tabulate the $\mathcal{I}$ and $\mathcal{W}$-eigenvalues for different choices of parameters $m$ and $\delta$ in Tab. VI. In this Section we set $\delta=0$, so the Hamiltonian is also time-reversal symmetric (TRS): $T\,h(k)\,T^{\text{-}1} = h(\text{-}k)$, with $T = i\Gamma_{20}K$; $K$ is the complex-conjugation operator. The two classes of TRS insulators are distinguished by a $\mathbb{Z}_2$ invariant $\Xi$, which is the change in time-reversal polarization over half an adiabatic cycle; $\Xi$ is odd for the nontrivial class.[86] In Fig. (3-a) and (3-b), we have plotted the $\mathcal{W}_{k_y}$-spectra for both $\mathbb{Z}_2$-trivial ($m=4.3$) and nontrivial ($m=3$) phases respectively.

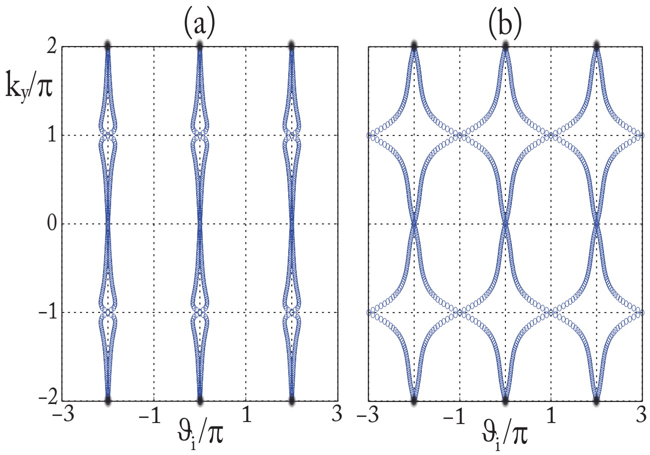

FIG. 3. The Wannier flow of a 2D insulator with both $\mathcal{I}$ and TR symmetries. (a) This phase has a trivial TR-invariant; it is realized in the model Hamiltonian (27), with parameters $m=4.3$, $\delta=0$. (b) This phase has a nontrivial TR-invariant; it is realized in the same model, with $m=3$, $\delta=0$.

| Parameter | | $\mathcal{I}$ eigenvalues | | | | $\mathcal{W}_{K_y}$ eigenvalues | |
|---|---|---|---|---|---|---|---|
| $m$ | $\delta$ | $(0,0)$ | $(\pi,0)$ | $(0,\pi)$ | $(\pi,\pi)$ | $K_y=0$ | $K_y=\pi$ |
| 3 | 0 | $(++)$ | $(++)$ | $(++)$ | $(--)$ | $[++]$ | $[--]$ |
| 3 | 1 | $(++)$ | $(++)$ | $(++)$ | $(--)$ | $[++]$ | $[--]$ |
| 3 | 2 | $(++)$ | $(++)$ | $(++)$ | $(--)$ | $[++]$ | $[--]$ |
| 4.3 | 0 | $(++)$ | $(++)$ | $(++)$ | $(++)$ | $[++]$ | $[++]$ |

TABLE VI. For various choices of the parameters $m,\delta$ in the Hamiltonian (27), we write the corresponding (a) $\mathcal{I}$ eigenvalues at the four symmetric momenta and (b) the eigenvalues of $\mathcal{W}_{K_y}$.

As derived in App. I, TRS imposes the following constraints on the $\mathcal{W}_{k_y}$ spectra:
(i) The sets of eigenvalues at $\pm k_y$ are equal, *i.e.*,

$$\big\{\exp i\vartheta_{k_y}\big\} = \big\{\exp i\vartheta_{\text{-}k_y}\big\}. \tag{28}$$

(ii) The $\mathcal{W}$'s at symmetric momenta satisfy

$$\mathcal{W}^{\text{-}1}_{K_y} = \Theta^{\text{-}1}\,\mathcal{W}_{K_y}\,\Theta, \tag{29}$$

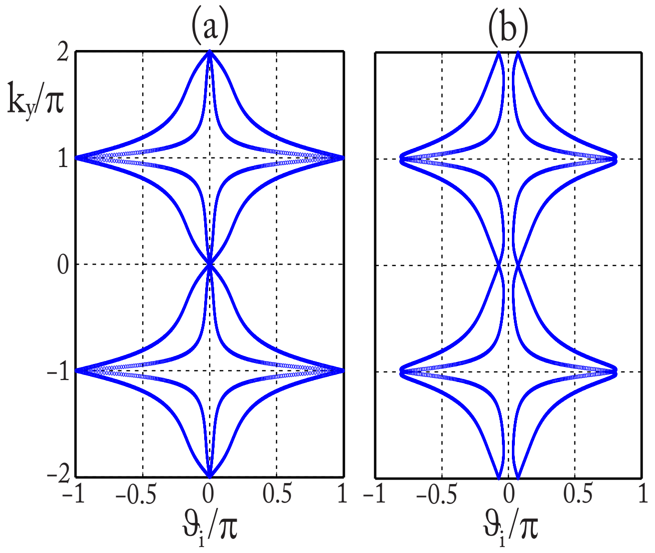

FIG. 4. (a) An $\mathcal{I}$-symmetric phase with relative winding $W = 2$; spectral flow is protected by $\mathcal{I}$ symmetry alone. This is the ground state of Hamiltonian (31). (b) Spectral flow is interrupted with an $\mathcal{I}$-breaking perturbation.

with $\Theta$ an antiunitary operator that squares to $-I$. This implies that every eigenstate of $\mathcal{W}_{K_y}$ has a degenerate Kramer's partner. (i) and (ii) imply that if one Wannier center produces a Hall current $I_H$, its Kramer's partner produces a time-reversed current that cancels $I_H$. As shown in Ref. 57 and 67, the $\mathbb{Z}_2$ invariant may be extracted from Fig. (3) in the following manner: in the region $k_y \in [0,\pi]$, $\vartheta \in [-\pi,\pi]$, let us draw a constant-$\vartheta$ reference line at any value of $\vartheta$. If the Wannier trajectories intersect this reference line an odd number of times, the phase is nontrivial, and vice versa.

By imposing $\mathcal{I}$ symmetry as well, we arrive at the following conclusions:

(a) Due to $\mathcal{I}$ symmetry, the $\mathcal{W}_{K_y}$-spectra at $K_y = \{0,\pi\}$ consist of $\pm 1$ and complex-conjugate pairs; the additional constraint of Kramer's degeneracy implies that the spectra is composed of *pairs* of [+1, +1], *pairs* of [-1, -1] and complex-conjugate *quartets* $[\lambda\,\lambda\,\lambda^*\lambda^*]$. Since time-reversal and $\mathcal{I}$ commute, the two states in a Kramer's doublet must transform in the same representation under $\mathcal{I}$ – this limits the possible $\mathcal{I}$ eigenvalues in a TRS ground state.

(b) From (25) and (28) we derive

$$\{\exp i\vartheta_{k_y}\} = \{\exp\text{-}i\vartheta_{\text{-}k_y}\} = \{\exp i\vartheta_{\text{-}k_y}\}, \tag{30}$$

which indicates that the flow of the Wannier centers in one quadrant, say $\vartheta \in [0,\pi]$ and $k_y \in [0,\pi]$, determines the flow in the full range, $\vartheta \in [-\pi,\pi]$ and $k_y \in [-\pi,\pi]$, by reflections. This is illustrated in Fig. (3), where each quadrant is bounded by dotted lines.

### D. Inversion-Protected Spectral Flow and the Relative Winding Number

The Chern insulator and the TRS topological insulator exhibit spectral flow in the $\mathcal{W}$-spectrum; the symmetries that protect spectral flow are, respectively, charge conservation and time-reversal symmetry. In this Section, we report spectral flow of a third kind, which is protected by $\mathcal{I}$ symmetry alone. In our first example, we consider the eight-band model

$$\begin{aligned} h(k) = {} & (-1-\cos k_x-\cos k_y)\,\Theta_{030} + \sin k_x\,(\Theta_{310}+\Theta_{110}) \\ & + \sin k_y\,(\Theta_{210}+\Theta_{020}) + 0.8\sin k_x\,(\Theta_{311}+\Theta_{111}), \end{aligned} \tag{31}$$

with matrices $\Theta_{ijk}$ defined as $\sigma_i \otimes \tau_j \otimes \gamma_k$; $\sigma_{i=1,2,3}$ are Pauli matrices in spin space; for $i,j = \{1,2,3\}$, $\tau_i \otimes \gamma_j$ are products of Pauli matrices in a four-dimensional orbital space; $\sigma_0$ ($\tau_0 \otimes \gamma_0$) is the identity in spin (orbital) space. This Hamiltonian is $\mathcal{I}$-symmetric: $\Theta_{030}\,h(k)\,\Theta_{030} = h(\text{-}k)$, and time-reversal symmetric: $T\,h(k)\,T^{\text{-}1} = h(\text{-}k)$; here $T = i\Theta_{200}\,K$, and $K$ implements complex conjugation. The Fermi energy is chosen so that there are four occupied bands in the ground state. We tabulate the $\mathcal{I}$ and $\mathcal{W}$-eigenvalues in Tab. VII, and also plot the $\mathcal{W}_{k_y}$-spectrum in Fig. 4-a. With TRS, $C_1 = 0$. The change in time-reversal polarization over half an adiabatic cycle is 2 (even), hence the TR invariant is trivial.[86] Yet, Wannier trajectories interpolate across the full unit cell: $\vartheta \in [0,2\pi)$. Let us softly break $\mathcal{I}$ symmetry, while maintaining TRS, with the perturbation: $0.4\,\cos k_x\,\Theta_{022} + 0.4\,\cos k_y\,\Theta_{112}$. As evidence that spectral flow persists only with $\mathcal{I}$ symmetry, we find in Fig. 4-b that the spectrum is now gapped.

| $\mathcal{I}$ eigenvalues | | | | $\mathcal{W}_{K_y}$ eigenvalues | |
|---|---|---|---|---|---|
| $(0,0)$ | $(\pi,0)$ | $(0,\pi)$ | $(\pi,\pi)$ | $K_y=0$ | $K_y=\pi$ |
| $++++$ | $++++$ | $++++$ | $----$ | $++++$ | $----$ |

TABLE VII. For the Hamiltonian (31), we write the (a) $\mathcal{I}$ eigenvalues at the four symmetric momenta and (b) the eigenvalues of $\mathcal{W}_{K_y}$.

$\mathcal{I}$-protected spectral flow is characterized by a nonzero relative winding number $W$, which is defined in the following way. Two Wannier trajectories are said to wind relative to each other if they (i) intersect the *same* atomic site at a symmetric time $K_y$, then (ii) separate and intersect *adjacent* mid-bond sites half a period later ($K_y + \pi$). $W$ is defined as the number of stable pairs of relatively-winding trajectories. To make this definition precise, we outline a procedure to identify $W$:

(a) Count the number of Wannier trajectories that *directly* connect mid-bond and atomic sites in the quadrant $\{\vartheta \in [0,\pi], k_y \in [0,\pi]\}$; call this number $n_1$. By a direct connection, we mean a smooth trajectory that flows without interruption. We consider three examples:

in Fig. 5-a (blue) and 5-b (blue), $n_1 = 0$; $n_1 = 2$ in Fig. 4-a.

(b) Count the number of trajectories that directly connect mid-bond and atomic sites in another quadrant $\{\vartheta \in [-\pi, 0), k_y \in [0, \pi]\}$; call this $n_2$. In all three examples, $n_1 = n_2$.

(c) $W$ is the minimum of $\{n_1, n_2\}$. We find that the insulator of Fig. 4-a has relative winding $W = 2$; $W = 0$ in the other two cases.

For each pair of relatively-winding trajectories, one of the pair ( $\vartheta_1(k_y)$ ) has winding number +1 on the torus $\{\vartheta \in [\text{-}\pi, \pi), k_y \in [\text{-}\pi, \pi)\}$, and the other has winding -1. In principle, it is possible that $\vartheta_1(k_y)$ has winding $2n$+1 ($n \in \mathbb{Z}^+$), while its partner $\vartheta_2(k_y)$ has winding -$2n$-1. However, $n > 0$ implies that the trajectories $\vartheta_1(k_y)$ and $\vartheta_2(k_y)$ cross at a non-symmetric momentum ($k_y \neq \{0, \pi\}$); such degeneracies are not protected by symmetry - by a ground-state deformation that preserves both the energy gap and $\mathcal{I}$ symmetry, we may turn crossings into anti-crossings and thus reduce $n$ to 0. Since $W$ is the number of *stable* relatively-winding pairs, we eliminate all such accidental degeneracies *before* carrying out the above procedure to identify $W$. All accidental degeneracies fall into two categories: (i) at non-symmetric momenta, there may be accidental crossings of two or more trajectories, as illustrated in Fig. 5-b (red). A slight deformation results in level repulsion, and turns crossings into anticrossings (Fig. 5-b (blue)). (ii) At symmetric momenta $\{0, \pi\}$, we rule out complex-conjugate-pair eigenvalues that are degenerate at either the atomic or mid-bond site. In the example of Fig. 5-a (red), there is one such degeneracy at the atomic site when $K_y = 0$, and another at the mid-bond site when $K_y = \pi$; upon perturbing the Hamiltonian, this degeneracy splits, as shown in Fig. 5-a (blue).

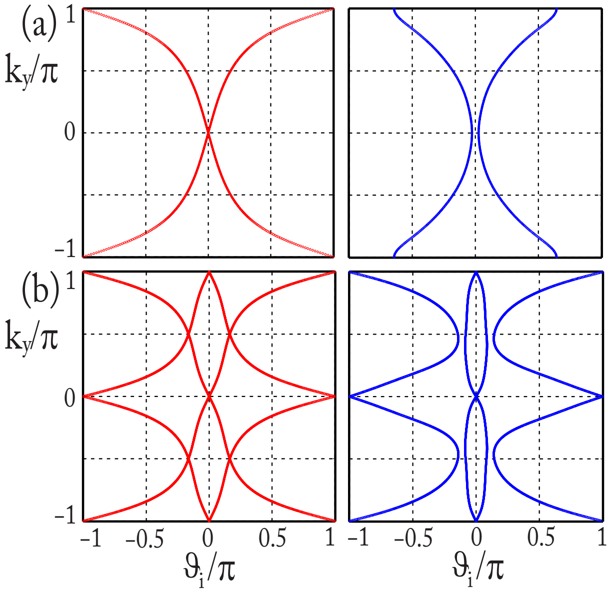

FIG. 5. Figures in red provide two examples of accidental degeneracies. Upon a gap- and symmetry-preserving perturbation, these accidental degeneracies split, as shown in blue.

Let us derive a sufficient condition for relative winding, and simultaneously relate $W$, $C_1$ and the eigenvalues of $\mathcal{W}$ at constant $K_y = \{0, \pi\}$. We define $N_{(+1)}(K_y)$, $N_{(-1)}(K_y)$ and $N_{(cc)}(K_y)$ as the number of +1,-1 and complex-conjugate-pair eigenvalues of $\mathcal{W}_{K_y}$, respectively; $N_{(+1)}(K_y) + N_{(-1)}(K_y) + N_{(cc)}(K_y) = n_{occ}$, the number of occupied bands. Define the quantity $N_d$ as in Eq. (2); if $N_d > 0$, there are $N_d$ trajectories that directly connect the mid-bond site (at $K_y$) and the atomic site (at $K_y + \pi$); otherwise, there are none. Of these $N_d$ trajectories, one or more pairs may relatively wind, and the rest wind with center-of-mass motion, thus contributing to the Chern number $C_1$. The parity of $C_1$ is constrained as in (26). A sufficient condition for relative winding is that $|C_1| < N_d$, in which case $2W = N_d - |C_1|$. If $|C_1| \geq N_d$, then $W = 0$. For $\mathcal{I}$- and time-reversal-symmetric (I+TRS) insulators, $C_1 = 0$, hence the relative winding is related to $N_d$ through: $2W = N_d$. These relations, as summarized in Tab. II, also imply that $W$ is isotropic, in the following sense. We define $\{\varphi(k_x)\}$ as Wannier trajectories of the Wilson loop at constant $k_x$; if $\{\vartheta(k_y)\}$ exhibits relative winding $W$, then so will $\{\varphi(k_x)\}$. This claim is substantiated in App. J.

### 1. *Relative Winding of Insulators with both Inversion and Time-Reversal Symmetries*

In this Section we study the relative winding of insulators with both $\mathcal{I}$ and TRS (I+TRS); we shall relate the relative winding $W$ with the TR invariant $\Xi$. While both $W$ and $\Xi$ characterize Wannier trajectories with no center-of-mass motion, they differ in many important respects. For I+TRS insulators with *nonzero* relative winding, the parity of $W$ determines the TR invariant: $\Xi = W$ mod 2; $\Xi$ is odd in the nontrivial class. To prove this, we apply the rule: modulo 2, $\Xi$ equals the number of Wannier trajectories that intersect a constant-$\vartheta$ reference line.[57] With I+TRS, only one quadrant, e.g. $\{\vartheta \in [0, \pi], k_y \in [0, \pi]\}$, is independent. In the rest of this section, we denote coordinates in this quadrant by $(\vartheta, k_y)$. Two cases are possible: (i) $W$ number of trajectories directly connect points $(\vartheta, k_y) = (\pi, 0)$ and $(0, \pi)$, or (ii) $W$ trajectories connect $(\pi, \pi)$ and $(0, 0)$. If $n_{occ} = 2W$, there are exactly $W$ intersections with the reference line, hence $\Xi = W$ mod 2. If $n_{occ} > 2W$, it is possible in case (i) that: (i-a) an extra trajectory connects $(0, 0)$ and $(0, \pi)$, (i-b) a trajectory connects $(\pi, 0)$ and $(\pi, \pi)$, (i-c) if there exists a complex-conjugate quartet $[\lambda_1 \lambda_1 \lambda_1^* \lambda_1^*]$ in the spectrum of $\mathcal{W}_{K_y=0}$, a pair of trajectories may connect $(0, \pi)$ with the complex-conjugate site at $(\lambda_1, 0)$, and (i-d) if there exists a complex-conjugate quartet $[\lambda_2 \lambda_2 \lambda_2^* \lambda_2^*]$ in the spectrum of $\mathcal{W}_{K_y=\pi}$, a pair of trajectories may connect $(\pi, 0)$ with the complex-conjugate site $(\lambda_2, \pi)$. In all scenarios, these extra trajectories intersect an even number of times with the reference line – the parity of the number of intersections is decided by $W$ alone. The proof is complete.

While only the parity of $W$ matters to the $\mathbb{Z}_2$ classification under TRS, $W$ provides a $\mathbb{Z}$ classification under $\mathcal{I}$ symmetry, and hence a more complete characterizaton. This distinction may be understood from a stability analysis of the Wannier centers. Since Kramer's degeneracy is two-fold, four or more Wannier centers generically experience level repulsion. Consider for example the $W = 2$, I+TRS model of Fig. 4-a. Sitting at the atomic site (at $K_y = \pi$) are four Wannier centers which are constrained by $\mathcal{I}$-symmetry – they do not experience level repulsion. If we now break $\mathcal{I}$-symmetry while preserving TRS, these four Wannier centers destabilize and split to form two pairs of Kramer's doublets, thus breaking spectral flow; see Fig. 4-b.

For I+TRS insulators with zero relative winding, it is possible that spectral flow is completely absent and the insulator is trivial. However, an I+TRS insulator with four or more occupied bands may have a nontrivial TR invariant without relative winding. To distinguish these two cases, we look to the indices $N_{(\text{-}1)}(0)$ and $N_{(\text{-}1)}(\pi)$. Since $W = 0$, all $N_{(\text{-}1)}(K_y)$ Wannier centers that originate from the mid-bond site (at $K_y$) must flow to either a complex-conjugate site or a mid-bond site (at $K_y + \pi$). By conservation of trajectories, $N_{(\text{-}1)}(K_y) - N_{(\text{-}1)}(K_y + \pi)$ number of trajectories must connect the mid-bond site (at $K_y$) to complex-conjugate sites (at $K_y + \pi$); here we have assumed $N_{(\text{-}1)}(K_y) > N_{(\text{-}1)}(K_y + \pi)$. Since $C_1 = 0$, we know from (26) that $N_{(\text{-}1)}(K_y) - N_{(\text{-}1)}(K_y + \pi)$ is even – within one quadrant, e.g., $\{\vartheta \in [0, \pi],\ k_y \in [K_y, K_y{+}\pi]\}$, $(N_{(\text{-}1)}(K_y){-}N_{(\text{-}1)}(K_y{+}\pi))/2$ number of trajectories connect the mid-bond site (at $K_y$) to complex-conjugate sites (at $K_y + \pi$). Two cases arise: (i) if $(N_{(\text{-}1)}(K_y) - N_{(\text{-}1)}(K_y + \pi))/2$ is *odd*, there must be at least *one other* trajectory that interpolates between $K_y$ and $K_y + \pi$. Then the sum of all trajectories that connect to complex-conjugate sites is *even*, as required by Kramer's degeneracy. Hence, TRS enforces a zig-zag pattern of Wannier flows, as illustrated schematically in Fig 6-a and -b. (ii) For even $(N_{(\text{-}1)}(K_y) - N_{(\text{-}1)}(K_y + \pi))/2$, Kramer's degeneracy is satisfied without additional trajectories, and the resultant Wannier flows are gapped, as in Fig. 6-c and -d. Therefore,

$$\begin{aligned} \Xi &= \tfrac{1}{2}\left(\, N_{(\text{-}1)}(0) - N_{(\text{-}1)}(\pi) \,\right) \mod 2 \\ &= \tfrac{1}{2}\, N_d \mod 2; \end{aligned} \tag{32}$$

for the last equality, we applied the definition of $N_d$ in Eq. (2) and that $N_{(cc)}(K_y)$ is a multiple of four; *c.f.* Sec. III C. The relation (32) applies to I+TRS insulators with $W > 0$ as well, since we have proven $\Xi = W$ mod 2 in this Section, and previously identified $2W = N_d$ in Sec. III D. The relations between $\Xi$, $W$ and $N_d$ are summarized in Tab. II.

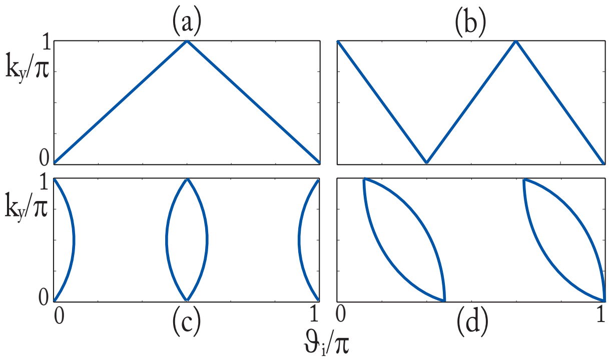

FIG. 6. Schematic illustrations of wannier flows with zero relative winding. In figures (a) and (b), $\frac{1}{2}(N_{(\text{-}1)}(0) - N_{(\text{-}1)}(\pi)) = 1$ (odd); the Wannier trajectories follow a zig-zag pattern. (c) $\frac{1}{2}(N_{(\text{-}1)}(0) - N_{(\text{-}1)}(\pi)) = 0$ (even), and the Wannier flows are gapped. (d) $\frac{1}{2}(N_{(\text{-}1)}(0) - N_{(\text{-}1)}(\pi)) = 2$ (even).

Consider for example the eight-band model:

$$\begin{aligned} h(k) = &\left(\, -2 - \ \cos k_x - \ \cos k_y \,\right) \Theta_{033} + \tfrac{4}{5}\ \cos k_y\, \Theta_{001} \\ &+ 5 \sin k_x \left(\Theta_{113} + \Theta_{313}\right) - \tfrac{3}{2} \sin k_y \left(\Theta_{020} + \Theta_{210}\right) \\ &+ \left(\, 6 \sin k_x + \tfrac{7}{2}\ \sin k_y \,\right) \left(\, \Theta_{023} + \Theta_{213} \,\right) + \Theta_{030}, \end{aligned} \tag{33}$$

with matrices $\Theta_{ijk}$ defined in (31). This Hamiltonian has the same symmetries as that in (31), namely $\mathcal{I}$ and TRS, and the ground state is defined to be the four lowest-energy bands. We tabulate the $\mathcal{I}$ and $\mathcal{W}$-eigenvalues in Tab. VIII. As illustrated in Fig. 7-a, the relative winding is trivial, but partner-switching occurs with help from the complex-conjugate quartet at $K_y = 0$. In this $W = 0$ model, spectral flow is protected by TRS alone. As evidence, we deform the Hamiltonian with a TRS-breaking term, $\Delta h(k) = 8 \sin k_x \left(\, \Theta_{022} + \Theta_{120} + \Theta_{121} \,\right) + 2 \sin k_y\, \Theta_{123}$, which preserves both the energy gap and $\mathcal{I}$ symmetry. As illustrated in Fig. 7-b, Kramer's degeneracy is now lifted – the quartet $[\lambda\lambda\lambda^*\lambda^*]$ at $K_y = 0$ splits into two separate doublets $[\lambda_1\, \lambda_1^*]$, $[\lambda_2\, \lambda_2^*]$. This contrasts with a previous example, where we broke TRS in a $\Xi$-nontrivial phase; as shown in Fig. 1-b, the resultant $\mathcal{W}$-spectrum is not gapped, due to a nonzero relative winding.

| $\mathcal{I}$ eigenvalues | | | | $\mathcal{W}_{K_y}$ eigenvalues | |
|---|---|---|---|---|---|
| $(0,0)$ | $(\pi,0)$ | $(0,\pi)$ | $(\pi,\pi)$ | $K_y = 0$ | $K_y = \pi$ |
| $++--$ | $++--$ | $++--$ | $----$ | $\lambda\,\lambda\,\lambda^*\lambda^*$ | $++--$ |

TABLE VIII. For the Hamiltonian (33), we write the (a) $\mathcal{I}$ eigenvalues at the four symmetric momenta and (b) the eigenvalues of $\mathcal{W}_{K_y}$.

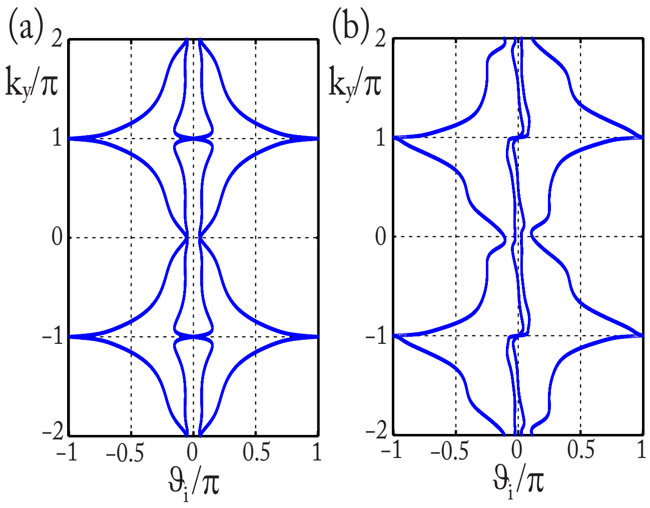

FIG. 7. (a) An $\mathcal{I}$-symmetric phase with zero relative winding; spectral flow persists due to TRS alone. This is the ground state of Hamiltonian (33). (b) Spectral flow is interrupted with a TRS-breaking perturbation.

## IV. CONCLUSION

In this paper we have developed a topological classification of inversion-symmetric insulators (ISI) based on the Wilson loop. We propose to classify the 1D ISI with an index $N_{\text{(-1)}} \in \mathbb{Z}$, which coincides with the number of protected boundary modes in the entanglement spectrum.[48,71] In 2D, we identify an invariant $W$ that characterizes spectral flow in the Wilson-loop spectrum; $W$ provides a $\mathbb{Z}$ classification of the 2D ISI. In contrast, $W$ has no analogs in both the entanglement and physical energy spectra, where there exists no spectral flow that is protected by inversion symmetry alone. A theory to formulate $N_{\text{(-1)}}$ and $W$ as topological obstructions to certain gauges remains to be developed; the experimental verification of these invariants also remains an open question. Inversion is but the simplest point-group symmetry – we may ask how the Wilson-loop spectrum is influenced by other point-group symmetries, *e.g.*, $C_n$.

*Acknowledgements* AA is grateful to Taylor L. Hughes, Chen Fang, Wu Yangle, Alexey Soluyanov and Edward Witten for illuminating discussions. AA was supported by the First Year Fellowship at Princeton University and NSF CAREER DMR-095242. XD was supported by NSF of China and the 973 program of China (No. 2007CB925000). BAB was supported by Princeton Startup Funds, NSF CAREER DMR-095242, ONR - N00014-11-1-0635 and NSF-MRSEC DMR-0819860 at Princeton University. This work was also supported by DARPA under SPAWAR Grant No.: N66001-11-1-4110.

### Appendix A: Derivation of parallel transport equation (8)

Let us define $u^n_k$ as eigenfunctions of the flat-band Hamiltonian $\mathcal{H}_{\text{F}}(k)$, with energy $\varepsilon_{\text{-}}$; the Hamiltonian is derived in Eq. (7). $n$ is a band index that runs over the occupied bands, and $k$ labels the crystal momentum. $u^n_k$ form basis vectors in the subspace of occupied bands. Upon adiabatic evolution through the Brillouin zone, the state $u^n_{k^{(i)}}$ at some initial momentum $k^{(i)}$ (at time $t_i$) is mapped to a different state $v^n_k$ at final momentum $k$ (at time $t$). In this process, the state acquires a dynamical phase $\int_{t_i}^t \varepsilon_{\text{-}} dt$. In addition, there is a unitary rotation of basis vectors in the occupied subspace; this rotation is affected by a $U(n_{occ})$ Wilson-line matrix $\mathcal{W}_{k\leftarrow k^{(i)}}$:

$$v^n_k(r) = e^{-i\int_{t_i}^t \varepsilon_{\text{-}} dt} \sum_{m=1}^{n_{occ}} u^m_k(r)\, \mathcal{W}^{mn}_{k\leftarrow k^{(i)}} \tag{A1}$$

In the adiabatic approximation, $v^n_k$ remains an eigenstate of the $\mathcal{H}_{\text{F}}(k)$ with energy $\varepsilon_{\text{-}}$. Let us apply the time-dependent Schrodinger equation and sum over repeated indices:

$$\varepsilon_{\text{-}}\, v^n_k(r) = \mathcal{H}_{\text{f}}(k)\, v^n_k(r) = i\partial_t\big[e^{-i\int_{t_i}^t \varepsilon_{\text{-}} dt}\, u^m_k(r)\, \mathcal{W}^{mn}_{k\leftarrow k^{(i)}}\big]. \tag{A2}$$

Upon cancellation of the dynamical phase and replacing $\partial_t = \sum_{\mu=1}^d (dk_\mu/dt)\,\partial_{k_\mu}$ for a $d$-dimensional BZ, we arrive at Eq. (8).

### Appendix B: Properties of Wilson loops

In this Appendix we derive several properties of Wilson loops, which apply to both continuum and tight-binding versions, as defined in Sec. I A and I C respectively. The derivations have been carried out with the tight-binding connection $A_k$ (*cf.* Eq. (14) ) and for a 1D BZ; they are trivially generalizable to the continuum connection $C_k$ (*cf.* Eq. (9) ) and to higher dimensions.
(i) Let us denote a Wilson line, over a path with start point $k^{(i)}$ and end point $k^{(f)}$, as $\mathcal{W}_{k^{(f)}\leftarrow k^{(i)}}$. The Wilson line between two infinitesimally-separated momenta is $\mathcal{W}^{mn}_{k+\epsilon\leftarrow k} = \big\langle U^m_{k+\epsilon}\big|U^n_k\big\rangle$. Let us define loop $\mathcal{L}$ as tracing a path between base point $k^{(0)}$ and end point $k^{(0)} + 2\pi$; we divide the $\mathcal{L}$ into infinitesimally-separated momenta: $\{k^{(0)} + 2\pi, k^{(N)}, k^{(N\text{-}1)} \ldots k^{(2)}, k^{(1)}, k^{(0)}\}$, with $N \gg 1$. Let $\mathcal{P}_k = \sum_{m=1}^{n_{occ}} \big|U^m_k\big\rangle\big\langle U^m_k\big|$ denote the projection to the occupied bands at momentum $k$. The Wilson loop may be discretized: $[\mathcal{W}(\mathcal{L})]^{mn}$

$$\begin{aligned}&= \mathcal{W}^{ml}_{k^{(0)}+2\pi\leftarrow k^{(N)}}\, \mathcal{W}^{lq}_{k^{(N)}\leftarrow k^{(N\text{-}1)}} \ldots\, \mathcal{W}^{op}_{k^{(2)}\leftarrow k^{(1)}}\, \mathcal{W}^{pn}_{k^{(1)}\leftarrow k^{(0)}} \\ &= \big\langle U^m_{k^{(0)}+2\pi}\big|\, \mathrm{T}\prod_{\alpha=1}^{N} \mathcal{P}_{k_\alpha}\, \big|U^n_{k^{(0)}}\big\rangle. \end{aligned} \tag{B1}$$

The product of projections are path-ordered (symbolized by T) along $\mathcal{L}$, with the earlier-time momenta positioned to the right.

(ii) Let $\mathcal{C}$ be a path that connects two arbitrary momenta $k^{(1)}$ and $k^{(2)}$, and $\mathcal{C}^T$ be the same path with opposite path-ordering. The Wilson line satisfies the unitary condition

$$\mathcal{W}_{k^{(2)}\leftarrow k^{(1)}}(\mathcal{C})^{\dagger} = \mathcal{W}_{k^{(1)}\leftarrow k^{(2)}}(\mathcal{C}^T) = \mathcal{W}_{k^{(2)}\leftarrow k^{(1)}}(\mathcal{C})^{\text{-}1}. \tag{B2}$$

For $k^{(2)} = k^{(1)} + 2\pi$, the above relation generalizes to Wilson loops. From (B2) one can derive that for a fixed loop, the eigenspectrum of $\mathcal{W}$ is independent of the base point.

(iv) Under a $U(n_{occ})$ gauge transformation, the product of projections in Eq. (B1) is invariant, but the eigenfunctions at the base and end points transform as $\big|U^n_{k^{(0)}}\big\rangle \rightarrow \sum_m \big|U^m_{k^{(0)}}\big\rangle\, M^{mn}(k^{(0)})$. Hence, the Wilson loop transforms as $\mathcal{W} \rightarrow M^{\dagger}(k^{(0)})\,\mathcal{W}\,M(k^{(0)})$, and the eigenspectrum of $\mathcal{W}$ is gauge-invariant.

## Appendix C: Wilson Loops and the Projected Position Operator

Let us demonstrate that the phases of the $\mathcal{W}$-spectrum coincide with the eigenspectrum of the projected position operator $\mathcal{P}^{\text{occ}}\,\hat{x}\,\mathcal{P}^{\text{occ}}$.[114] Here, $\mathcal{P}^{\text{occ}}$ projects to the occupied subspace of the translationally-invariant Hamiltonian (5), which have Bloch eigenfunctions $\psi^n_k(x) = e^{ikx}\,u^n_k(x)$. We are interested in eigenfunctions $\Psi$ that satisfy

$$\big(\,\mathcal{P}^{\text{occ}}\,\hat{x}\,\mathcal{P}^{\text{occ}} - \tfrac{1}{2\pi}\,\vartheta\,\big)\;\Psi(x) = 0 \tag{C1}$$

for some eigenvalue $\vartheta/2\pi$. We expand $\Psi$ in the subspace of occupied Bloch waves:

$$\Psi(x) = \sum_{n=1}^{n_{occ}} \int \tfrac{dk}{2\pi}\; f_{nk}\; \psi^n_k(x). \tag{C2}$$

In the periodic gauge ($\psi^n_k = \psi^n_{k+2\pi}$), the action of the projected position operator on the wavefunction $f$ may be decomposed into an intra-band operator $\partial_k$ and an inter-band operator $C$:[120]

$$\big\langle \psi^n_k\big|\; \mathcal{P}^{\text{occ}}\,\hat{x}\,\mathcal{P}^{\text{occ}}\; \big|\Psi\big\rangle = i\,\frac{\partial f_{nk}}{\partial k} + i\sum_{m=1}^{n_{occ}}\,[C(k)]^{nm}\,f_{mk}, \tag{C3}$$

where $C$ is the non-Abelian connection that is defined in (9). In the general solution to (C1), the wavefunctions at two different momenta ($k$ and $k^{(i)}$) are related by the Wilson line

$$f_{mk} = e^{-i(k\text{-}k^{(i)})\vartheta/2\pi} \sum_{n=1}^{n_{occ}} \Big[\,\mathrm{T}\; e^{\text{-}\int_{k^{(i)}}^{k}\, C(q)\,dq}\,\Big]^{mn}\, f_{nk^{(i)}}. \tag{C4}$$

It follows from the periodic boundary condition on $f$ that

$$\sum_{n=1}^{n_{occ}} \mathcal{W}^{mn}_{k+2\pi\leftarrow k}\; f_{nk} = e^{i\vartheta}\; f_{m,k+2\pi} = e^{i\vartheta}\; f_{m,k}, \tag{C5}$$

hence we have shown that the eigenspectrum of $\mathcal{P}^{\text{occ}}\,\hat{x}\,\mathcal{P}^{\text{occ}}$ coincides with the phases of the eigenspectrum of $\mathcal{W}$. Furthermore, let us derive the eigenfunctions of $\mathcal{P}^{\text{occ}}\,\hat{x}\,\mathcal{P}^{\text{occ}}$. Define the $U(n_{occ})$ matrix $Q(k)$ such that its columns are the eigenstates of the Wilson loop at base point $k$: $\mathcal{W}_{k+2\pi\leftarrow k}$. That is, $\mathcal{W}_{k+2\pi\leftarrow k} = Q(k)\,D\,Q^{\dagger}(k)$, where $D$ is a diagonal matrix that contains the eigenvalues of $\mathcal{W}$. While the eigenvalues of $\mathcal{W}$ do not depend on the base point $k$, the eigenfunctions $Q(k)$ do. The matrix $Q(k)$ is related to the matrix $Q(k' \neq k)$ by a Wilson line:

$$\begin{aligned}&\mathcal{W}_{k'+2\pi\leftarrow k'} = \mathcal{W}^{\dagger}_{k\leftarrow k'}\;\mathcal{W}_{k+2\pi\leftarrow k}\;\mathcal{W}_{k\leftarrow k'}\\ &\quad\Rightarrow\;\; Q(k') = \mathcal{W}^{\dagger}_{k\leftarrow k'}\;Q(k) = \mathcal{W}_{k'\leftarrow k}\;Q(k).\end{aligned} \tag{C6}$$

We label the $j$'th diagonal element in $D$ by $\exp\big(\,i\vartheta^{(j)}\,\big)$, where $j$ runs from $1, 2\,\ldots\,n_{occ}$. If $\vartheta^{(j)}/2\pi$ is an eigenvalue of $\mathcal{P}^{\text{occ}}\,\hat{x}\,\mathcal{P}^{\text{occ}}$, so is any integer addition to $\vartheta^{(j)}/2\pi$, as is consistent with $\vartheta^{(j)}$ being a phase. For each occupied band, there exists an infinite ladder of eigenvalues: $\vartheta^{(j)}_R/2\pi = \vartheta^{(j)}/2\pi + R\,; R \in \mathbb{Z}$. The index $R$ labels the unit cell where the eigenfunction is localized. We will choose the convention that $\text{-}\pi < \vartheta^{(j)} \leq \pi$. Let us then label the eigenfunctions of $\mathcal{P}^{\text{occ}}\,\hat{x}\,\mathcal{P}^{\text{occ}}$ by $j = 1\,\ldots\,n_{occ}$ and $R \in \mathbb{Z}$. The wavefunction $[f^{(j)}_R]_{n,k} \propto Q(k)_{nj}$ so as to satisfy the eigenvalue equation (C5). In addition, we multiply the $j$'th column of the eigenmatrix $Q(k)$ by a momentum-dependent phase, so as to ensure periodicity:

$$\begin{aligned}[f^{(j)}_R]_{n,k+2\pi} &= e^{-i(k+2\pi)\vartheta^{(j)}_R/2\pi}\;Q(k+2\pi)_{nj}\\ &= e^{-i(k+2\pi)\vartheta^{(j)}_R/2\pi}\sum_{m=1}^{n_{occ}}\mathcal{W}^{nm}_{k+2\pi\leftarrow k}\;Q(k)_{mj}\\ &= e^{-i(k+2\pi)\vartheta^{(j)}_R/2\pi}\;e^{i\vartheta^{(j)}}\;Q(k)_{nj} = [f^{(j)}_R]_{n,k}.\end{aligned} \tag{C7}$$

In the second equality, we have applied the relation (C6). In summary, to each eigenvalue $\vartheta^{(j)}_R/2\pi$ there corresponds an eigenfunction of $\mathcal{P}^{\text{occ}}\,\hat{x}\,\mathcal{P}^{\text{occ}}$:

$$\Psi^{(j)}(x\text{-}R) = \sum_{n=1}^{n_{occ}} \int \tfrac{dk}{2\pi}\; e^{\text{-}ik\,(\frac{\vartheta^{(j)}}{2\pi}+R)}\; Q(k)_{nj}\;\psi^n_k(x). \tag{C8}$$

## Appendix D: The Tight-Binding Formalism and the Relation between the Full and Tight-Binding Connections

In the tight-binding variational approximation, the Hilbert space is reduced to $n_{tot}$ atomic orbitals $\phi_{\alpha}(r-R)$ on each lattice site ($R$); $\phi_{\alpha}$ are eigenstates of an atomic Hamiltonian $H_{\text{atom}}$, and $\alpha = 1, 2, \ldots, n_{tot}$ is an orbital/spin index. Due to the finite overlap of atomic orbitals on different lattice sites, we are motivated to construct an orthonormal basis that preserves the point-group symmetries of $\phi_\alpha$. Such a basis is realized with Löwdin functions,[117–119] which are defined as

$$\varphi_\alpha(x-R_i) = \sum_{j,\beta} \phi_\beta(x-R_j)\ [\Delta^{\text{-}1/2}]^{\beta\alpha}_{ji} \tag{D1}$$

with the hermitian overlap integral

$$\Delta^{\alpha\beta}_{ij} = \int d^{\mathrm{d}}r\ \phi^*_\alpha(x-R_i)\ \phi_\beta(x-R_j) = \Delta^{\beta\alpha *}_{ji}. \tag{D2}$$

Here, $i,j$ are indices for lattice sites; we sum over repeated indices. The orthogonality of Löwdin function reads as

$$\int d^d r\, \varphi^*_\alpha(x-R)\, \varphi_\beta(x-R') = \delta_{\alpha\beta}\, \delta_{R,R'}. \tag{D3}$$

Let us define the operator $\hat{I}$ by its action on functions: $\hat{I}\, f(r) = f(\text{-}r)$. If the atomic Hamiltonian preserves $\mathcal{I}$ symmetry, *i.e.* $[H_{\text{atom}}, \hat{I}] = 0$, then one may define a Hermitian, unitary, $n_{tot} \times n_{tot}$ sewing matrix $\wp$ in the basis of atomic orbitals:

$$\wp_{\alpha\beta} = \int d^d r\ \phi^*_\alpha(r)\, \hat{I}\, \phi_\beta(r) = \langle \phi_\alpha |\, \hat{I}\, | \phi_\beta \rangle. \tag{D4}$$

The Löwdin functions $\varphi$, which are constructed from $\phi$ through (D1), transform identically under point-group symmetry operations,[117] hence $\hat{I}\, \varphi_\alpha(r) = \varphi_\alpha(\text{-}r) = \varphi_\delta(r)\, \wp_{\delta\alpha}$ as well. In Hamiltonians with discrete translational symmetry, we form the Bloch sums

$$u_{k\alpha}(r) = \tfrac{1}{\sqrt{N}} \sum_R e^{-ik(r-R)} \varphi_\alpha(r-R), \tag{D5}$$

which are periodic in lattice translations. The tight-binding Hamiltonian (*cf.* (13)) is defined as

$$\begin{aligned}
[h(k)]_{\alpha\beta} &= \langle u_{k\alpha} |\ \mathcal{H}(k)\ | u_{k\beta} \rangle \\
&= \sum_R e^{-ikR} \int d^{\mathrm{d}}r\ \varphi^*_\alpha(r-R) \big[\tfrac{p^2}{2m} + V(r)\big] \varphi_\beta(r)
\end{aligned} \tag{D6}$$

In the tight-binding approximation, the periodic component of the Bloch wave $\psi^n_k$ is

$$u^n_k(r) = \frac{1}{\sqrt{N}} \sum_{R\alpha} e^{-ik(r-R)}\, [U^n_k]_\alpha\, \varphi_\alpha(r-R), \tag{D7}$$

where $[U^n_k]_\alpha$ is the unitary eigenmatrix that diagonalizes (D6). Let us relate the full connection $C_k$ (cf. (9)) to the tight-binding connection $A_k$ (cf. (14)). By inserting (D7) into (9), we obtain (17), where we have defined $\hat{r}_\mu$ as the position operator in the basis of occupied bands:

$$\begin{aligned}
[r_\mu]^{nm}_k = \tfrac{1}{N}\, [U^n_k]^*_\beta\, [U^m_k]_\alpha \sum_{R,R'} e^{ik(R-R')} \\
\times \int d^{\mathrm{d}}r\ \varphi^*_\beta(r-R')\, r_\mu\, \varphi_\alpha(r-R),
\end{aligned} \tag{D8}$$

and $\bar{R}_\mu = \sum_R R_\mu/N$ is the average atomic displacement in the direction $\mu$. One can prove that the connections $A$ and $C$ are anti-Hermitian, while the position operator $r_\mu$ is Hermitian. Under a $U(n_{occ})$ gauge transformation, $U^m_k \to U^j_k M^{jm}(k)$, the matrix $[r_\mu]_k$ undergoes a unitary transformation $[r_\mu]_k \to M(k)[r_\mu]_k M(k)^{\text{-}1}$ – thus, the eigenspectrum of $r_\mu$ is gauge-invariant.

## Appendix E: Analytic Properties of the Sewing Matrix and Constraints on the Wilson Loop due to Inversion Symmetry

Let us employ the bra-ket notation that is introduced in Sec. I C. As defined in Eq. (19), the sewing matrix links occupied eigenstates $U^n_k$ of the tight-binding Hamiltonian at $\pm k$: $B^{mn}_k = [U^m_{\text{-}k}]^*_\alpha\ \wp_{\alpha\beta}\ [U^n_k]_\beta = \langle U^m_{\text{-}k} |\ \wp\ | U^n_k \rangle$; $\wp$ is an overlap matrix that is defined in Eq. (18). Here, $m,n$ are indices that label the occupied bands. We choose a gauge in which, at inversion-invariant momenta, $B_{k^{\text{inv}}}$ is a diagonal matrix with diagonal elements equal to the $\mathcal{I}$ eigenvalues of $U^n_{k^{\text{inv}}}$. We prove that $B_k$ is unitary. Let us label the unoccupied bands by the primed index $m' = n_{occ}{+}1, \ldots, n_{\text{tot}}$. If the ground state is insulating, *i.e.*, $\langle U^{m'}_{\text{-}k} |\ \wp\ | U^n_k \rangle = 0$ for all $n$ occupied bands and all $m'$ unoccupied bands,

$$\sum_{m=1}^{n_{occ}} B^{mn}_k\, B^{ml*}_k = \sum_{m=1}^{n_{occ}} \langle U^m_{\text{-}k} | \wp | U^n_k \rangle \langle U^m_{\text{-}k} | \wp | U^l_k \rangle^* = \sum_{m=1}^{n_{\text{tot}}} \langle U^l_k | \wp | U^m_{\text{-}k} \rangle \langle U^m_{\text{-}k} | \wp | U^n_k \rangle = \langle U^l_k |\, \wp^2\, | U^n_k \rangle = \delta^{ln}. \tag{E1}$$

In the second equality, we have used the identity: $\langle U^{m'}_{\text{-}k} |\ \wp\ | U^n_k \rangle = 0$; the third equality required the completeness relation. Furthermore, the Hermicity of the inversion operation $\wp$ implies $B_{\text{-}k} = [B_k]^\dagger = B^{\text{-}1}_k$. Applying (19) and $\wp^2 = I$, we derive the following condition for a Wilson line between two infinitesimally-separated momenta $k^{(1)}$ and

$k^{(2)}$:

$$\mathcal{W}^{mn}_{\text{-}k^{(2)}\leftarrow\text{-}k^{(1)}} = \big\langle U^m_{\text{-}k^{(2)}} \big| U^n_{\text{-}k^{(1)}} \big\rangle = B^{mo}_{k^{(2)}} \, \big\langle U^o_{k^{(2)}} \big| \, \wp^2 \, \big| U^l_{k^{(1)}} \big\rangle \, B^{nl*}_{k^{(1)}} = B^{mo}_{k^{(2)}} \, [\mathcal{W}_{A}]^{ol}_{k^{(2)}\leftarrow k^{(1)}} \, B^{nl*}_{k^{(1)}}. \tag{E2}$$

This relation is generalizable to a Wilson line between arbitrary momenta. We divide the finite path between $k^{(1)}$ and $k^{(2)}$ into infinitesimally-separated momenta: $\{k^{(1)}, k^{(1)}+\Delta, k^{(1)}+2\Delta, \ldots, k^{(2)}-\Delta, k^{(2)}\}$. Following Eq. (B1),

$$\begin{aligned} \mathcal{W}^{mn}_{k^{(2)}\leftarrow k^{(1)}} &= \mathcal{W}^{ml}_{k^{(2)}\leftarrow k^{(2)}-\Delta} \, \mathcal{W}^{lo}_{k^{(2)}-\Delta\leftarrow k^{(2)}-2\Delta} \cdots \mathcal{W}^{pn}_{k^{(1)}+\Delta\leftarrow k^{(1)}} \\ &= B^{mr}_{\text{-}k^{(2)}} \, \mathcal{W}^{rs}_{\text{-}k^{(2)}\leftarrow\text{-}k^{(2)}+\Delta} \, B^{ls*}_{\text{-}k^{(2)}+\Delta} \, B^{lt}_{\text{-}k^{(2)}+\Delta} \, \mathcal{W}^{tu}_{\text{-}k^{(2)}+\Delta\leftarrow\text{-}k^{(2)}+2\Delta} \, B^{ou*}_{\text{-}k^{(2)}+2\Delta} \cdots B^{pv}_{-\Delta} \, \mathcal{W}^{vw}_{\text{-}k^{(1)}-\Delta\leftarrow\text{-}k^{(1)}} \, B^{nw*}_{\text{-}k^{(1)}} \\ &= B^{mr}_{\text{-}k^{(2)}} \, \mathcal{W}^{rs}_{\text{-}k^{(2)}\leftarrow\text{-}k^{(2)}+\Delta} \, \mathcal{W}^{so}_{\text{-}k^{(2)}+\Delta\leftarrow\text{-}k^{(2)}+2\Delta} \cdots \mathcal{W}^{pw}_{\text{-}k^{(1)}-\Delta\leftarrow\text{-}k^{(1)}} \, B^{nw*}_{\text{-}k^{(1)}} = B^{mr}_{\text{-}k^{(2)}} \, \mathcal{W}^{rs}_{\text{-}k^{(2)}\leftarrow\text{-}k^{(1)}} \, B^{ns*}_{\text{-}k^{(1)}}. \end{aligned} \tag{E3}$$

Applying this result to a Wilson loop between -$\pi$ and $\pi$,

$$\mathcal{W}^{mn}_{\pi\leftarrow\text{-}\pi} = B^{mr}_{\text{-}\pi} \, \mathcal{W}^{rs}_{\text{-}\pi\leftarrow\pi} \, B^{ns*}_{\pi} = B^{mr}_{\text{-}\pi} \, \mathcal{W}^{\dagger rs}_{\pi\leftarrow\text{-}\pi} \, B^{ns*}_{\pi} = B^{mr}_{\text{-}\pi} \, \mathcal{W}^{\dagger rs}_{\pi\leftarrow\text{-}\pi} \, [B^{sn}_{\text{-}\pi}]^{\dagger}. \tag{E4}$$

Here we have used the identities (B2) and $B_{k^{\text{inv}}} = B^{\dagger}_{k^{\text{inv}}}$. (E4) informs us that $\mathcal{W}$ is equivalent to its Hermitian adjoint through a unitary transformation, hence we derive (20) for $\mathcal{W}$. Let us apply (E3) to derive (21):

$$\mathcal{W}^{mn}_{\pi\leftarrow\text{-}\pi} = \mathcal{W}^{ml}_{\pi\leftarrow 0} \, \mathcal{W}^{ln}_{0\leftarrow\text{-}\pi} = B^{mr}_{\pi} \, \mathcal{W}^{\dagger rs}_{0\leftarrow\text{-}\pi} \, B^{sl}_{0} \, \mathcal{W}^{ln}_{0\leftarrow\text{-}\pi}, \tag{E5}$$

We have derived (20) and (21) for the tight-binding Wilson loop ( *cf.* (15) ), for which the connection involves tight-binding eigenfunctions $U^n_k$. Similar results apply to the continuum Wilson loop ( *cf.* (1) ), for which the connection involves $u^n_k$ – eigenfunctions of the Bloch Hamiltonian (6). We may similarly define a $U(n_{occ})$ sewing matrix: $\bar{B}^{mn}_k = \int d^d r \; u^{m*}_{\text{-}k}(r) \, u^n_k(\text{-}r)$ that links Bloch eigenfunctions at $\pm k$. Within the tight-binding approximation, we may relate $u^n_k$ and $U^n_k$ through (D7), and identify $\bar{B}$ as identical to the sewing matrix $B$ of (19). This identity implies that the mapping between $\mathcal{I}$ and $\mathcal{W}$ eigenvalues, as presented in Sec. II B, applies to both tight-binding and continuum Wilson loops. If the ground state is characterized by $n_s = 0$ ($n_s$ is defined in Sec. II B), the spectra of both Wilson loops are identical, and comprise only $\pm 1$ eigenvalues. If $n_s > 0$, the spectra of both Wilson loops comprise the same numbers of $\pm 1$ and complex-conjugate-pair eigenvalues; they may differ only in the phases of the complex eigenvalues.

## Appendix F: Case Studies of the 1D Inversion-Symmetric Insulator

### 1. Case Study: 1 Occupied Band

With one occupied band, there is only one Wannier center per unit cell. In each unit cell, the Wannier center can only be at a atomic site or at a mid-bond site; only these spatial configurations in a periodic lattice are invariant under inversion. If the Bloch waves at $k = 0$ and $\pi$ transform under different representations of $\mathcal{I}$, $\mathcal{W}$ = -1. Proof: We shall employ notation that is defined in (21). Being unitary, $\mathcal{W}_{\,0\leftarrow\text{-}\pi}$ must be of the form $\exp(i\vartheta)$. (21) informs us that $\mathcal{W}(\mathcal{L}) = B_\pi \exp(\text{-}i\vartheta) \, B_0 \exp(i\vartheta) = B_\pi \, B_0$, which is a product of the $\mathcal{I}$ eigenvalues of the sole occupied band at $k = 0$ and $\pi$. The proof is complete. This result can be verified by a model tight-binding Hamiltonian

$$h(k) = -(\alpha + \cos k) \, \tau_3 + \sin k \; \tau_2, \tag{F1}$$

with $\tau_i$ defined as Pauli matrices in orbital space. This Hamiltonian has an $\mathcal{I}$ symmetry: $\tau_3 \, h(k) \, \tau_3 = h(\text{-}k)$; the insulator is trivial when $\alpha > 1$, and nontrivial when -1 $< \alpha < 1$.

### 2. Case Study: 2 Occupied Bands

For $\mathcal{I}$-symmetric insulators with two occupied bands, $\mathcal{W}$ is a $2 \times 2$ matrix; our case study captures many qualitative features of larger-dimensional $\mathcal{W}$'s. We assume a general form for $\mathcal{W}_{\,0\leftarrow\text{-}\pi}$ that satisfies unitarity:

$$\mathcal{W}_{\,0\leftarrow\text{-}\pi} = e^{i\alpha} \begin{pmatrix} c & d \\ \text{-}d^* & c^* \end{pmatrix} \;\; ; \;\; |c|^2 + |d|^2 = 1. \tag{F2}$$

Inserting (F2) into (21), we arrive at $\mathcal{W}(\mathcal{L}) =$

$$\begin{pmatrix} \xi^1_\pi \big(|c|^2 \xi^1_0 + |d|^2 \xi^2_0\big) & c^* d \, \xi^1_\pi \big(\xi^1_0 - \xi^2_0\big) \\ c d^* \, \xi^2_\pi \big(\xi^1_0 - \xi^2_0\big) & \xi^2_\pi \big(|c|^2 \xi^2_0 + |d|^2 \xi^1_0\big) \end{pmatrix}, \tag{F3}$$

where $\xi^1_{k^{\text{inv}}}$ and $\xi^2_{k^{\text{inv}}}$ are diagonal elements of the sewing matrix $B_{k^{\text{inv}}}$. We exhaust the possible $\mathcal{I}$ eigenvalues $\{\xi_{k^{\text{inv}}}\}$, solve the characteristic equations and derive the $\mathcal{W}$ spectra. Our results are tabulated in Tab. IV.

Cases (i)-(iii) of Tab. IV may be summarized as: if the $\mathcal{I}$ eigenvalues of occupied bands at either $k = 0$ or $\pi$ are identical, *i.e.*, if either sewing matrix $B_0$ or $B_\pi$ is proportional to the identity, then the $\mathcal{W}$-spectrum comprises only $\pm 1$ eigenvalues; its eigenvalues are the diagonal elements of the product $B_0 \, B_\pi$.

| Model parameters | | $\mathcal{I}$ eigenvalues | | $\mathcal{W}$ |
|---|---|---|---|---|
| $\alpha$ | $\beta$ | 0 | $\pi$ | spectrum |
| 0 | 0 | $(++)$ | $(++)$ | $[++]$ |
| 1.5 | 0 | $(+-)$ | $(++)$ | $[+-]$ |
| 1.5 | -1.5 | $(--)$ | $(++)$ | $[--]$ |
| 1.5 | 1.5 | $(+-)$ | $(+-)$ | $[\lambda\lambda^*]$ |

TABLE IX. A model of an $\mathcal{I}$-symmetric ground state with two occupied bands: for various choices of the parameters $\alpha, \beta$ in the Hamiltonian (F4), we write the corresponding $\mathcal{I}$ and $\mathcal{W}$-eigenvalues.

In case (iv) of Tab. IV, we encounter (a) occupied bands with nonidentical $\mathcal{I}$ eigenvalues at both $k = 0$ and $\pi$, and (b) a complex-conjugate pair of $\mathcal{W}$-eigenvalues $(\lambda\lambda^*)$: a pair of Wannier centers are positioned equidistantly on opposite sides of each atomic site. The exact position is not determined by symmetry; this arbitrariness reflects the range in this equivalence class of $\mathcal{I}$-symmetric insulators, *i.e.*, it is possible to tune the Hamiltonian and sweep the interval of allowed $\lambda$ while preserving both the insulating gap and $\mathcal{I}$ symmetry. This implies that case (iv) is trivial. Why? Let us tune the Hamiltonian to a limit in which bands of identical representation are fully coupled, *i.e.*, the positive-$\mathcal{I}$ (negative-$\mathcal{I}$) band at $k = \text{-}\pi$ adiabatically evolves into the positive-$\mathcal{I}$ (negative-$\mathcal{I}$) at 0, through the Wilson line $\mathcal{W}_{0\leftarrow\text{-}\pi}$. For example, if $\xi_0^1 = \xi_\pi^2 = \text{-}\xi_\pi^1 = \text{-}\xi_0^2$, the two $\mathcal{W}$-eigenvalues are $|d|^2 - |c|^2 \pm 2i|c||d|$. Tuning $|c| \rightarrow 0$ and $|d| \rightarrow 1$ effectively decouples the two-band $\mathcal{W}$ into two one-band $\mathcal{W}$'s; each Abelian $\mathcal{W}$ connects bands of the same representation between $k = 0$ and $\pi$, hence each contributes +1 to the spectrum, and $\mathcal{W} \rightarrow I$. As discussed in the Introduction, if $\mathcal{W}$ is tunable to the identity, then the insulator is in the same equivalence class as the atomic insulator, hence we conclude that case (iv) is trivial.

In contrast with complex-conjugate-pair $\mathcal{W}$-eigenvalues, protected -1 eigenvalues obstruct $\mathcal{W}$ from being tuned to the identity. The nontrivial insulators are cases (ii) and (iii) of Tab. IV, which have one and two -1 eigenvalues respectively. We distinguish between case (iii) and the degenerate limit of case (iv), in which $\mathcal{W} \rightarrow \text{-}I$; this is the limit in which bands of identical representation are fully decoupled, *i.e.*, the positive-$\mathcal{I}$ (negative-$\mathcal{I}$) band at $k = \text{-}\pi$ adiabatically evolves into the negative-$\mathcal{I}$ (positive-$\mathcal{I}$) at 0. In case (iii), the equality $\mathcal{W} = \text{-}I$ is robust against gap- and symmetry-preserving transformations of the ground-state, while this is not true in case (iv).

Let us verify our results in Tab. IV with the model, tight-binding Hamiltonian

$$\begin{aligned} h(k) &= -\Gamma_{03} + 0.1\,\Gamma_{13} + (\Gamma_{21} + \Gamma_{31})\sin k \\ &\quad + \tfrac{1}{2}\big(\,\alpha\,(\Gamma_{30} + \Gamma_{03}) + \beta\,(\Gamma_{30} - \Gamma_{03})\,\big)\cos k, \end{aligned} \tag{F4}$$

with matrices $\Gamma_{ij}$ defined as $\sigma_i \otimes \tau_j$; $\sigma_0$ ($\tau_0$) is the identity in spin (orbital) space; $\sigma_{i=1,2,3}$ ($\tau_{i=1,2,3}$) are Pauli matrices in spin (orbital) space. The Hamiltonian is $\mathcal{I}$-symmetric: $\Gamma_{03}\,h(k)\,\Gamma_{03} = h(\text{-}k)$. The Fermi energy is chosen so that there are two occupied bands in the ground state. We tabulate the $\mathcal{W}$ spectra for various choices of the parameters $\alpha$ and $\beta$ in Tab. IX.

## Appendix G: Proof of mapping between $\mathcal{I}$ and $\mathcal{W}$ eigenvalues

We employ notation that has been defined in Sec. II B: $n_{(\pm)}(k^{\text{inv}})$, FBOS, $k_s, \xi_s, n_s$. As defined in Eq. (19), $B_k$ is a $U(n_{occ})$ sewing matrix linking bands at $\pm k$ through $\mathcal{I}$. At symmetric momenta $k^{\text{inv}}$, a gauge is chosen in which $B_{k^{\text{inv}}}$ is a diagonal matrix with elements $\{\xi_1(k^{\text{inv}}), \xi_2(k^{\text{inv}}), \ldots, \xi_{n_{occ}}(k^{\text{inv}})\}$ equal to the $\mathcal{I}$ eigenvalues at $k^{\text{inv}}$. At momentum $k_s$, we pick a convention that the fewest bands of one symmetry (FBOS) are indexed by $m = 1, 2, \ldots, n_s$ and the rest of the bands at $k_s$ are indexed by $m = n_s$+$1, \ldots, n_{occ}$. We evaluate the Wilson loop $\mathcal{W}$ over a path that begins at $k_s$-$\pi$, sweeps the interval $[k_s\text{-}\pi, k_s + \pi]$ and ends at $k_s + \pi$; the $\mathcal{W}$-spectrum is independent of the base point, as shown in App. B. In the rest of the section, we simplify notation and assume that $\mathcal{W} = \mathcal{W}_{k_s+\pi\leftarrow k_s\text{-}\pi}$. Let us reproduce a result presented in (21): $\mathcal{W} = B_{k_s+\pi}\,Z^\dagger\,B_{k_s}\,Z$, with $Z$ defined as the Wilson line $\mathcal{W}_{k_s\leftarrow k_s\text{-}\pi}$; $Z^{-1} = Z^\dagger$. Let us define $Y$ as the $n_{occ} \times n_{occ}$ matrix

$$Y = \tfrac{1}{2}\big(I + \xi_s\,B_{\pi+k_s}\,\mathcal{W}\big). \tag{G1}$$

Since $B^2_{\pi+k_s} = I$, the matrix elements of $Y$ are

$$Y_{ij} = \tfrac{1}{2}\big(I + \xi_s\,Z^\dagger\,B_{k_s}\,Z\big)_{ij} = \sum_{l=1}^{n_s} Z^*_{li}\,Z_{lj}. \tag{G2}$$

Here we have applied the unitarity condition $Z^\dagger Z = I$ to express $[Z^\dagger B_{k_s} Z]_{ij} = \sum_{a=1}^{n_{occ}} \xi_a(k_s)\,Z^*_{ai}\,Z_{aj} = \text{-}\xi_s(\delta_{ij} - 2\sum_{b=1}^{n_s} Z^*_{bi}\,Z_{bj})$. We deduce from (G2) that $Y$ is a rank-$n_s$ projection matrix. If $n_s = 0$, $Y$ is the zero matrix. We define $\bar{Y}^{\alpha_1\alpha_2\ldots\alpha_m}$ as $m \times m$ submatrices in $Y$ that lie on the intersections of rows numbered by $\{\alpha_1, \alpha_2, \ldots, \alpha_m\}$ with columns numbered by $\{\alpha_1, \alpha_2, \ldots, \alpha_m\}$. For example, $\bar{Y}^1 = \sum_{a=1}^{n_s} Z^*_{a,1}\,Z_{a,1}$, and

$$\bar{Y}^{23} = \begin{pmatrix} \sum_{a=1}^{n_s} Z^*_{a,2}\,Z_{a,2} & \sum_{a=1}^{n_s} Z^*_{a,2}\,Z_{a,3} \\ \sum_{a=1}^{n_s} Z^*_{a,3}\,Z_{a,2} & \sum_{a=1}^{n_s} Z^*_{a,3}\,Z_{a,3} \end{pmatrix}. \tag{G3}$$

The determinant of a $m \times m$ submatrix $\bar{Y}$ is also called the $m \times m$ minor of $Y$. According to a well-known theorem in linear algebra, the rank of a matrix is equal to the largest integer $r$ for which a nonzero $r \times r$ minor exists, therefore det $\bar{Y}^{\alpha_1\alpha_2\ldots\alpha_m} = 0$ if $m > n_s$. Applying (G1), the characteristic equation $\det[\lambda\,I - \mathcal{W}] = 0$ is equivalent to

$$\begin{aligned} 0 &= \det[\,\text{-}\xi_s\,B_{k_s+\pi}\,]\,\det[\,\lambda\,I - \mathcal{W}\,] \\ &= \det[\,(\text{-}\xi_s\,\lambda\,B_{k_s+\pi} - I) + 2\,Y\,] \end{aligned} \tag{G4}$$

We claim that the determinant in the second line of (G4) is equal to a polynomial in $\lambda$ of order $2n_s$, multiplied by the factor $(-\xi_s\,\lambda-1)^{[n_{(+)}(k_s+\pi)-n_s]}\,(\xi_s\,\lambda-1)^{[n_{(-)}(k_s+\pi)-n_s]}$, where $n_{(+)}(k_s+\pi)$ $(n_{(-)}(k_s+\pi))$ is the number of positive-$\mathcal{I}$ (negative-$\mathcal{I}$) bands at $k_s+\pi$. Upon proving this claim, we deduce that there are $(n_{(+)}(k_s+\pi)-n_s)$ number of $-\xi_s$ $\mathcal{W}$-eigenvalues and $(n_{(-)}(k_s+\pi)-n_s)$ number of $+\xi_s$ $\mathcal{W}$-eigenvalues. Furthermore, we apply a result presented in (20): the $\mathcal{W}$-eigenvalues can either be $\pm 1$ or form complex-conjugate pairs $\lambda,\lambda^*$. Thus, the zeros of the polynomial $R(\lambda)$ correspond to $n_s$ complex-conjugate pairs of eigenvalues.

*Proof*:

We define $\lambda_i = -\xi_s\,\xi_i(k_s+\pi)\,\lambda$. By a binomial-like expansion, we express the characteristic equation as:

$$0=\sum_{m=0}^{n_{occ}} 2^m \sum_{\{\alpha_1,\alpha_2\ldots\alpha_m\}} \det \bar{Y}^{\alpha_1\alpha_2\ldots\alpha_m} \prod_{i=1;i\neq\alpha_1,\alpha_2\ldots\alpha_m}^{n_{occ}} (\lambda_i\text{-}1). \tag{G5}$$

The sum $\sum_{\{\alpha_1,\alpha_2\ldots\alpha_m\}}$ runs over the $n_{occ}$ choose $m$ combinations of the indices $\{\alpha_1\ldots\alpha_m\}$. An example of the characteristic equation for an insulator with 4 occupied bands is

$$\begin{aligned}0=&(\lambda_1-1)(\lambda_2-1)(\lambda_3-1)(\lambda_4-1)+\Big[2\,\bar{Y}^1(\lambda_2-1)(\lambda_3-1)(\lambda_4-1)+8\,\det\,[\bar{Y}^{123}]\;(\lambda_4-1)+\text{comb. }1\Big]\\&+\Big[4\,\det\,[\bar{Y}^{12}]\;(\lambda_3-1)(\lambda_4-1)+\text{comb. }2\Big]+16\,\det\,[\bar{Y}^{1234}]\end{aligned} \tag{G6}$$

where $[f(1234)+\text{ comb. }1]=f(1234)+f(4123)+f(3412)+f(2341)$ and $[f(1234)+\text{comb. }2]=f(1234)+f(1324)+f(1423)+f(2314)+f(2413)+f(3412)$. Applying the rank-minor theorem, only the first $n_s$+1 terms in (G5) are nonzero:

$$0=\sum_{m=0}^{n_s} 2^m \sum_{\{\alpha_1,\alpha_2\ldots\alpha_m\}} \det \bar{Y}^{\alpha_1\alpha_2\ldots\alpha_m} \prod_{i=1;i\neq\alpha_1,\alpha_2\ldots\alpha_m}^{n_{occ}} (\lambda_i\text{-}1). \tag{G7}$$

Let us organize this expansion. We first consider a term in (G7) with a particular combination of $m$ band indices given by the set $\{\alpha_1\ldots\alpha_m\}$ in the superscript of $\bar{Y}$. Each band index $\alpha_i$ has a corresponding $\mathcal{I}$ eigenvalue $\xi_{\alpha_i}$ at $k=k_s+\pi$; in this set we may define $m_+$ $(m_-)$ as the number of positive (negative) $\mathcal{I}$ eigenvalues in the set $\{\xi_{\alpha_1}(k_s+\pi)\ldots\xi_{\alpha_m}(k_s+\pi)\}$; note $m_++m_-=m$. The *presence* of each band $\alpha_i$ in this set implies that a factor of $(-\xi_s\,\xi_{\alpha_i}(k_s+\pi)\,\lambda\text{-}1)$ is *absent* in the product $\prod_{i=1;i\neq\alpha_1,\alpha_2\ldots\alpha_m}^{n_{occ}}(\lambda_i\text{-}1)$. In the remainder of this proof, we use the convention that $\alpha_i$ $(\beta_i)$ are positive-$\mathcal{I}$ (negative-$\mathcal{I}$) band indices at $\pi+k_s$. We may organize the expansion by collecting terms with the same $m_+$:

$$0=\sum_{m=0}^{n_s} 2^m \sum_{m_+=0}^{m} \big(-\xi_s\lambda\text{-}1\big)^{[n_{(+)}(k_s+\pi)-m_+]}\,\big(\xi_s\lambda\text{-}1\big)^{[n_{(-)}(k_s+\pi)-m+m_+]}\;S_{m_+,m-m_+} \tag{G8}$$

with $S_{x,y}$ defined as the sum of all minors $\det\bar{Y}^{\alpha_1\ldots\alpha_{m_+}\beta_1\ldots\beta_{m_-}}$ with $m_+=x$ and $m_-=y$:

$$S_{x,y}=\sum_{\{\alpha_1\ldots\alpha_x\,\beta_1\ldots\beta_y\}} \det\bar{Y}^{\alpha_1\ldots\alpha_x\,\beta_1\ldots\beta_y}. \tag{G9}$$

By definition, there are $n_{(+)}(k_s+\pi)$ $(n_{(-)}(k_s+\pi))$ number of positive-$\mathcal{I}$ (negative-$\mathcal{I}$) bands at $k_s+\pi$, hence the sum $\sum_{\{\alpha_1\ldots\alpha_x\,\beta_1\ldots\beta_y\}}$ runs over $n_{(+)}(k_s+\pi)$ choose $x$ combinations of positive-$\mathcal{I}$ bands, multiplied by $n_{(-)}(k_s+\pi)$ choose $y$ combinations of negative-$\mathcal{I}$ bands. As the form of (G8) suggests, nonzero terms in the expansion have values of $m_+$ ranging from a minimum of 0 to a maximum of $n_s$. That the expansion (G7) includes nonzero terms with $m_+=n_s, m_-=0$ and nonzero terms with $m_+=0, m_-=n_s$ is a consequence of our construction: by definition of FBOS and $n_s$, both $n_{(+)}(k_s+\pi)$ and $n_{(-)}(k_s+\pi)\geq n_s$. We observe that:

(i) Terms in the expansion with $m_+=n_s, m_-=0$ are proportional to $(-\xi_s\,\lambda\text{-}1)^{[n_{(+)}(k_s+\pi)-n_s]}$ because $n_s$ factors of $(-\xi_s\,\lambda\,\xi_{\alpha_i}(k_s+\pi)\text{-}1)$ with $\xi_{\alpha_i}=+1$ are removed from the product $\prod(\lambda_i\text{-}1)$. All other terms in the expansion have greater powers of $(-\xi_s\,\lambda\text{-}1)$.

(ii) Similarly, terms in the expansion with $m_+=0, m_-=n_s$ are proportional to $(\xi_s\,\lambda\text{-}1)^{[n_{(-)}(k_s+\pi)-n_s]}$ and all other terms in the expansion have greater powers of $(\xi_s\,\lambda\text{-}1)$.

(i) and (ii) imply that the common factor of all terms in the expansion is $(-\xi_s\,\lambda\text{-}1)^{[n_{(+)}(k_s+\pi)-n_s]}\,(\xi_s\,\lambda\text{-}1)^{[n_{(-)}(k_s+\pi)-n_s]}$. The characteristic equation is thus expressible as

$$0=\big(-\xi_s\lambda\text{-}1\big)^{[n_{(+)}(k_s+\pi)-n_s]}\,\big(\xi_s\lambda\text{-}1\big)^{[n_{(-)}(k_s+\pi)-n_s]}\;R(\lambda) \tag{G10}$$

with $R(\lambda)$ a polynomial of order $2n_s$ – the claim is proven.

## Appendix H: Proof of Eq. (25)

Let $\mathcal{L}^{k_y}$ be a path in the constant-$k_y$ interval $[(\text{-}\pi,k_y),(\pi,k_y)]$; we choose the path-ordering convention that $k_x$ increases along the path $\mathcal{L}^{k_y}$. We define (i) the time-reversed path $\mathcal{T}\,\mathcal{L}^{k_y}$, which sweeps the same interval with opposite path-ordering (*i.e.*, decreasing $k_x$), and (ii) the $\mathcal{I}$-mapped path $\mathcal{E}\,\mathcal{L}^{k_y}$, which sweeps the interval $[(\text{-}\pi,\text{-}k_y),(\pi,\text{-}k_y)]$ with decreasing $k_x$. In combination, $\mathcal{E}\,\mathcal{T}\mathcal{L}^{k_y} = \mathcal{L}^{\text{-}k_y}$; this observation leads us to the following identity:

$$\begin{aligned}\mathcal{W}^{\dagger}(\mathcal{L}^{\text{-}k_y}) &= \mathcal{W}(\,\mathcal{T}\,\mathcal{L}^{\text{-}k_y}) = B_{\pi,k_y}\,\mathcal{W}(\,\mathcal{E}\,\mathcal{T}\,\mathcal{L}^{\text{-}k_y})\,B^{\dagger}_{\text{-}\pi,k_y}\\ &= B_{\pi,k_y}\,\mathcal{W}(\mathcal{L}^{k_y})\,B^{\dagger}_{\text{-}\pi,k_y}.\end{aligned} \tag{H1}$$

where $B_k$ are sewing matrices defined in Sec. II A. The first equality follows from (B2), the second from (E3). Since $B_{\pi,k_y} = B_{\text{-}\pi,k_y}$ is unitary, we have shown that $\mathcal{W}$ along $\mathcal{L}^{k_y}$ is equivalent to the Hermitian adjoint of $\mathcal{W}$ along $\mathcal{L}^{\text{-}k_y}$ by a unitary transformation, as advertised.

## Appendix I: Wilson Loop of the 2D Time-Reversal Symmetric Insulator

The time-reversal operator is written as $T = Q\,K$, with $Q^{-1} = Q^{\dagger}$ and $K$ the complex-conjugation operator. On spin-half single-particle states, $T^2 = -I$, which implies $Q^T = -Q$. We define a matrix that sews occupied Bloch bands at $\pm k$ through $T$: $V^{ij}_k = \langle U^i_{\text{-}k}\big|T\big|U^j_k\rangle$; $i,j = 1\ldots n_{occ}$. $Q^T = -Q$ implies $V^T_k = \text{-}V_{\text{-}k}$. By a similar proof as one presented in App. E, one can show that $V^{-1} = V^{\dagger}$, which implies $[U^i_{\text{-}k}]_{\alpha} = V^{ij*}_k\,Q_{\alpha\beta}\,[U^j_k]^*_{\beta}$. Applying this relation to a Wilson line between $\text{-}k^{(1)}$ and $\text{-}k^{(2)}$, which are infinitesimally apart:

$$\begin{aligned}&\mathcal{W}^{ij}_{\text{-}k^{(1)}\leftarrow\text{-}k^{(2)}} = \langle U^i_{\text{-}k^{(1)}}\big|U^j_{\text{-}k^{(2)}}\rangle\\ &= V^{il}_{k^{(1)}}\,Q^*_{\alpha\beta}\,[U^l_{k^{(1)}}]_{\beta}\,V^{jm*}_{k^{(2)}}\,Q_{\alpha\delta}\,[U^m_{k^{(2)}}]^*_{\delta}\end{aligned} \tag{I1}$$

$$\Rightarrow\;\; \mathcal{W}_{\text{-}k^{(1)}\leftarrow\text{-}k^{(2)}} = V_{k^{(1)}}\,\mathcal{W}^*_{k^{(1)}\leftarrow k^{(2)}}\,V^{\dagger}_{k^{(2)}} \tag{I2}$$

By employing (B1), the relation (I2) is generalizable to finite-length paths, with arbitrary $k^{(1)},k^{(2)}$. We recall the definitions of $\mathcal{L}^{k_y}$, $\mathcal{T}\,\mathcal{L}^{k_y}$, $\mathcal{E}\,\mathcal{L}^{k_y}$ and $\mathcal{E}\,\mathcal{T}\,\mathcal{L}^{k_y}$, as detailed in App. H.

$$\begin{aligned}\mathcal{W}^{\dagger}(\,\mathcal{L}^{\text{-}k_y}\,) &= \mathcal{W}(\,\mathcal{T}\,\mathcal{L}^{\text{-}k_y}\,) = V_{\pi,k_y}\,\mathcal{W}(\,\mathcal{E}\,\mathcal{T}\,\mathcal{L}^{\text{-}k_y}\,)^*\,V^{\dagger}_{\text{-}\pi,k_y}\\ &= V_{\pi,k_y}\,\mathcal{W}(\,\mathcal{L}^{k_y}\,)^*\,V^{\dagger}_{\pi,k_y}.\end{aligned} \tag{I3}$$

The first equality follows from (B2), the second from (E3) and the third from $\mathcal{E}\,\mathcal{T}\,\mathcal{L}^{k_y} = \mathcal{L}^{\text{-}k_y}$. Since $V_{\pi,k_y}$ is unitary, we have shown that $\mathcal{W}$ along $\mathcal{L}^{k_y}$ is equivalent to the transpose of $\mathcal{W}$ along $\mathcal{L}^{\text{-}k_y}$ by a unitary transformation, thus proving (28).(I3) may be written in a familiar form:

$$\mathcal{W}^{\text{-}1}(\mathcal{L}^{\text{-}k_y}) = \Theta^{\text{-}1}\;\mathcal{W}(\mathcal{L}^{k_y})\;\Theta \tag{I4}$$

with $\Theta = KV^{\dagger}_{\pi,k_y}$, and satisfying $\Theta^2 = \text{-}I$. This implies that each eigenstate of $\mathcal{W}_{K_y}$ at $K_y = \{0,\pi\}$ has a degenerate Kramer's partner.

## Appendix J: Isotropy of $W$

Let us define $\{\varphi(k_x)\}$ ($\{\vartheta(k_y)\}$) as Wannier trajectories of the Wilson loop at constant $k_x$ ($k_y$). In this Section we prove that if $\{\vartheta(k_y)\}$ has a relative winding of $W$, so will $\{\varphi(k_x)\}$. This follows because:
(i) The Chern number is an obstruction to a smooth gauge in the BZ, hence both sets of trajectories, $\{\vartheta(k_y)\}$ and $\{\varphi(k_x)\}$, must exhibit the same center-of-mass winding $C_1$.
(ii) Let $M_{(1)}(K_x)$, $M_{(\text{-}1)}(K_x)$ and $M_{(cc)}(K_x)$ respectively be the number of +1,-1 and complex-conjugate-pair eigenvalues of the Wilson loop at constant $K_x = \{0,\pi\}$; $M_{(1)}(K_x) + M_{(\text{-}1)}(K_x) + M_{(cc)}(K_x) = n_{occ}$, the number of occupied bands. We define

$$\begin{aligned}M_d = \max\big\{\; &M_{(\text{-}1)}(\pi) - M_{(\text{-}1)}(0) - M_{(cc)}(0),\\ &M_{(\text{-}1)}(0) - M_{(\text{-}1)}(\pi) - M_{(cc)}(\pi)\;\big\};\end{aligned} \tag{J1}$$

if $M_d > 0$ there are $M_d$ number of Wannier trajectories that directly connect the atomic site (at $K_x$) and the mid-bond site (at $K_x + \pi$); if $M_d \leq 0$ there are none. By applying the mapping of Sec. II B, it is possible to prove by exhaustion that $M_d = N_d$, where $N_d$ is defined in Eq. (2).

Given (i) and (ii), the relations between $W, C_1$ and $N_d$ in Tab. II imply that both sets of trajectories, $\{\vartheta(k_y)\}$ and $\{\varphi(k_x)\}$, have the same relative winding $W$.

---

[1] X.-G. Wen, *Quantum Field Theory of Many-body Systems* (Oxford University Press, USA, 2007).

[2] A. Hamma, R. Ionicioiu, and P. Zanardi, Phys. Lett. A, **337**, 22 (2004).

[3] M. Levin and X.-G. Wen, Phys. Rev. Lett., **96**, 110405 (2006).

[4] A. Kitaev and J. Preskill, Phys. Rev. Lett., **96**, 110404 (2006).

[5] H. Li and F. D. M. Haldane, Phys. Rev. Lett., **101**, 010504 (2008).

[6] N. Bray-Ali, L. Ding, and S. Haas, Phys. Rev. B, **80**, 180504(R) (2009).

[7] S. T. Flammia, A. Hamma, T. L. Hughes, and X.-G. Wen, Phys. Rev. Lett., **103**, 261601 (2009).

[8] A. Alexandradinata, T. L. Hughes, and B. A. Bernevig, arXiv:1108.2907.

[9] R. Thomale, A. Sterdyniak, N. Regnault, and B. A. Bernevig, Phys. Rev. Lett., **104**, 180502 (2010).

[10] R. Thomale, D. P. Arovas, and B. A. Bernevig, Phys. Rev. Lett., **105**, 116805 (2010).

[11] F. Pollmann and J. E. Moore, New J. Phys., **12**, 025006 (2010).

[12] L. Fidkowski, Phys. Rev. Lett., **104**, 130502 (2010).

[13] E. Prodan, T. L. Hughes, and B. A. Bernevig, Phys. Rev. Lett., **105**, 115501 (2010).

[14] N. Regnault, B. A. Bernevig, and F. D. M., Phys. Rev. Lett., **103**, 016801 (2009).

[15] F. D. M. Haldane, APS 2009 March Meeting Proceeding (unpublished).

[16] M. Kargarian and G. A. Fiete, Phys. Rev. B, **82**, 085106 (2010).

[17] A. M. Läuchli, E. J. Bergholtz, J. Suorsa, and M. Haque, Phys. Rev. Lett., **104**, 156404 (2010).

[18] A. M. Läuchli, E. J. Bergholtz, and M. Haque, New Journal of Physics, **12**, 075004 (2010).

[19] E. J. Bergholtz, M. Nakamura, and J. Suorsa, arXiv: 1006.3658v2.

[20] A. Sterdyniak, N. Regnault, and B. A. Bernevig, Phys. Rev. Lett., **106**, 100405 (2011).

[21] I. D. Rodriguez and G. Sierra, arXiv: 1007.5356.

[22] Z. Papic, B. A. Bernevig, and N. Regnault, arXiv: 1008.5087.

[23] M. Hermanns, A. Chandran, N. Regnault, and B. A. Bernevig, arXiv: 1009.4199.

[24] Z. Papic, N. Regnault, and S. D. Sarma, Phys. Rev. Lett., **80**, 201303 (2009).

[25] X.-L. Qi, H. Katsura, and A. W. W. Ludwig, arXiv: 1103.5437.

[26] J. Zhao, D. N. Sheng, and F. D. M. Haldane, arXiv:1103.0772.

[27] J. Schliemann, Phys. Rev. B, **83**, 115322 (2011).

[28] R. Thomale, B. Estienne, N. Regnault, and B. A. Bernevig, arXiv: 1010.4837.

[29] D. Poilblanc, Phys. Rev. Lett., **105**, 077202 (2010).

[30] A. M. Turner, F. Pollmann, and E. Berg, Phys. Rev. B, **83**, 075102 (2011).

[31] L. Fidkowski and A. Kitaev, Phys. Rev. B, **81**, 134509 (2010).

[32] H. Yao and X.-L. Qi, Phys. Rev. Lett., **105**, 080501 (2010).

[33] F. Pollmann, A. M. Turner, E. Berg, and M. Oshikawa, Phys. Rev. B, **81**, 064439 (2010).

[34] P. Calabrese and A. Lefevre, Phys. Rev. A, **78**, 032329 (2008).

[35] M. Fagotti, P. Calabrese, and J. E. Moore, Phys. Rev. B, **83**, 045110 (2011).

[36] G. M. J.-M. Stéphan and V. Pasquier, arXiv: 1104.2544.

[37] D. Poilblanc, Phys. Rev. B, **84**, 045120 (2011).

[38] F. Franchini, A. R. Its, V. E. Korepin, and L. A. Takhtajan, arXiv:1002.2931.

[39] C.-Y. Huang and F.-L. Lin, arXiv: 1104.1139.

[40] J. I. Cirac, D. Poilblanc, N. Schuch, and F. Verstraete, Phys. Rev. B, **83**, 245134 (2011).

[41] J. Dubail and N. Read, arXiv:1105.4808.

[42] Z. Liu, H.-L. Guo, V. Vedral, and H. Fan, Phys. Rev. A, **83**, 013620 (2011).

[43] X. Deng and L. Santos, arXiv: 1104.5157.

[44] S. Ryu and Y. Hatsugai, Phys. Rev. B, **73**, 245115 (2006).

[45] A. Sterdyniak, N. Regnault, and B. A. Bernevig, arxiv: 1006.5435.

[46] A. M. Turner, Y. Zhang, and A. Vishwanath, arxiv: 0909.3119 ().

[47] A. M. Turner, Y. Zhang, and A. Vishwanath, Phys. Rev. B, **82**, 241102 (2010).

[48] T. L. Hughes, E. Prodan, and B. A. Bernevig, Phys. Rev. B, **83**, 245132 (2011).

[49] F. D. M. Haldane, Phys. Rev. Lett., **61**, 2015 (1988).

[50] C. L. Kane and E. J. Mele, Phys. Rev. Lett., **95**, 226801 (2005).

[51] C. L. Kane and E. J. Mele, Phys. Rev. Lett., **95**, 146802 (2005).

[52] B.A. Bernevig and S.C. Zhang, Phys. Rev. Lett., **96**, 106802 (2006).

[53] K. G. Wilson, Phys. Rev. D, **10**, 2445 (1974).

[54] L. Fidkowski, T. S. Jackson, and I. Klich, arxiv:1101.0320.

[55] G. Baskaran and P. W. Anderson, Phys. Rev. B, **37**, 580 (1988).

[56] S. Ryu, C. Mudry, H. Obuse, and A. Furusaki, New J. Phys., **12**, 065005 (2010).

[57] R. Yu, X. L. Qi, A. Bernevig, Z. Fang, and X. Dai, Phys. Rev. B, **84**, 075119 (2011).

[58] S.-S. Lee and S. Ryu, Phys. Rev. Lett., **100**, 186807 (2008).

[59] A. P. Schnyder, S. Ryu, A. Furusaki, and A. W. W. Ludwig, Phys. Rev. B, **78**, 195125 (2008).

[60] F. Wilczek and A. Zee, Phys. Rev. Lett., **52**, 2111 (1984).

[61] M. V. Berry, Proc. R. Soc. Lond A, **392**, 45 (1984).

[62] J. Zak, Phys. Rev. Lett., **48**, 359 (1982).

[63] J. Zak, Phys. Rev. Lett., **62**, 2747 (1989).

[64] R. Leone, J. Phys. A: Math. Theor., **44**, 295301 (2011).

[65] A. Ekert, M. Ericsson, P. Hayden, H. Inamori, J. A. Jones, D. K. L. Oi, and V. Vedral, J. Mod. Opt., **47**, 2501 (2000).

[66] A. Recati, T. Calarco, P. Zanardi, J. I. Cirac, and P. Zoller, Phys. Rev. A, **66**, 0302309 (2002).

[67] A. A. Soluyanov and D. Vanderbilt, Phys. Rev. B, **83**, 235401 (2011).

[68] A. M. Turner, Y. Zhang, R. S. K. Mong, and A. Vishwanath, arxiv:1010.4335 ().

[69] L. Fu and C. L. Kane, Phys. Rev. B, **76**, 045302 (2007).

[70] I. Peschel, J. Phys. A:Math. Gen., **36**, L205 (2003).

[71] A. M. Turner, Y. Zhang, R. S. K. Mong, and A. Vishwanath, Phys. Rev. B, **85**, 165120 (2012).

[72] R. D. King-Smith and D. Vanderbilt, Phys. Rev. B, **47**, 1651 (1993).

[73] D. Vanderbilt and R. D. King-Smith, Phys. Rev. B, **48**, 4442 (1993).

[74] R. Resta, Rev. Mod. Phys., **66**, 899 (1994).

[75] I. Souza and a. D. V. J. Iniquez, Phys. Rev. B, **69**, 085106 (2004).

[76] E. J. Mele and P. Kral, Phys. Rev. Lett., **88**, 056803 (2002).

[77] L. F. E. Yaschenko and L. Resca, Phys. Rev. B, **58**, 1222 (1998).

[78] J. E. Sipe and J. Zak, Phys. Lett. A, **258**, 406 (1999).

[79] D. J. Thouless, M. Kohmoto, M. P. Nightingale, and M. den Nijs, Phys. Rev. Lett., **49**, 405 (1982).

[80] X.L. Qi, Y.S. Wu, and S.C. Zhang, Phys. Rev. B, **74**, 045125 (2006).

[81] E. Prodan, J. Math. Phys., **50**, 083517 (2009).

[82] S. Coh and D. Vanderbilt, Phys. Rev. Lett., **102**, 107603 (2009).

[83] J. Bellissard, A. Vanelst, and H. Schulz-Baldes, J. Math. Phys., **35**, 5373 (1994).

[84] Q. Niu, D. J. Thouless, and Y.-S. Wu, Phys. Rev. B, **31**, 3372 (1985).

[85] V. Gurarie, Phys. Rev. B, **83**, 085426 (2011).

[86] L. Fu and C. L. Kane, Phys. Rev. B, **74**, 195312 (2006).

[87] B. A. Bernevig, T. L. Hughes, and S.C. Zhang, Science, **314**, 1757 (2006).

[88] M. König, S. Wiedmann, C. Brüne, A. Roth, H. Buhmann, L. Molenkamp, X.-L. Qi, and S.-C. Zhang, Science, **318**, 766 (2007).

[89] X.-L. Qi, T. Hughes, and S.-C. Zhang, Phys. Rev. B, **78**, 195424 (2008).

[90] C. Wu, B.A. Bernevig, and S.C. Zhang, Phys. Rev. Lett., **96**, 106401 (2006).

[91] C. Xu and J. Moore, Phys. Rev. B, **73**, 045322 (2006).

[92] L. Fu, C. L. Kane, and E. J. Mele, Phys. Rev. Lett., **98**, 106803 (2007).

[93] J. E. Moore and L. Balents, Phys. Rev. B, **75**, 121306 (2007).

[94] S. Murakami, N. Nagaosa, and S.C. Zhang, Phys. Rev. Lett., **93**, 156804 (2004).

[95] R. Roy, Phys. Rev. B, **79**, 195321 (2009).

[96] R. Roy, Phys. Rev. B, **79**, 195322 (2009).

[97] Y. Ran, A. Vishwanath, and D.-H. Lee, Phys. Rev. Lett., **101**, 086801 (2008).

[98] D. Hsieh, D. Qian, L. Wray, Y. Xia, Y. S. Hor, R. J. Cava, and M. Z. Hasan, Nature, **452**, 970 (2008).

[99] E. Prodan, Phys. Rev. B, **80**, 125327 (2009).

[100] E. Prodan, J. Phys. A: Math. Theor., **42**, 082001 (2009).

[101] A. M. Essin, J. E. Moore, and D. Vanderbilt, Phys. Rev. Lett., **102**, 146805 (2009).

[102] J. Xiong, A. C. Petersen, D. Qu, R. J. Cava, and N. P. Ong, arXiv:1101.1315.

[103] G. H. Wannier, *Elements of Solid State Theory* (Cambridge U. P., Cambridge, England, 1959).

[104] E. E. Mendez and G. Bastard, Phys. Today, **46**, 34 (1993).

[105] R. Resta, J. Phys.: Condens. Matter, **12**, R107 (2000).

[106] G. Sundaram and Q. Niu, Phys. Rev. B, **59**, 14915 (1999).

[107] M. Chang and Q. Niu, J. Phys.: Condens. Matter, **20**, 193202 (2008).

[108] E. E. Mendez, F. Agullo-Rueda, and J. M. Hong, Phys. Rev. Lett., **60**, 2426 (1988).

[109] M. Raizen, C. Salomon, and Q. Niu, Phys. Today, **50(7)**, 30 (1997).

[110] Q. Niu, X.-G. Zhao, G. A. Georgakis, and M. G. Raizen, Phys. Rev. Lett., **76**, 24 (1996).

[111] M. B. Dahan, E. Peik, J. Reichel, Y. Castin, and C. Salomon, Phys. Rev. Lett., **76**, 4508 (1996).

[112] S. R. Wilkinson, C. F. Bharucha, K. W. Madison, Q. Niu, and M. G. Raizen, Phys. Rev. Lett., **76**, 4512 (1996).

[113] A. P. Schnyder, S. Ryu, A. Furusaki, and A. W. W. Ludwig, AIP Conf. Proc., **1134**, 10 (2009).

[114] S. Kivelson, Phys. Rev. B, **26**, 4269 (1982).

[115] N. Marzari and D. Vanderbilt, Phys. Rev. B, **56**, 12847 (1997).

[116] W. Kohn, Phys. Rev., **115**, 809 (1959).

[117] J. Slater and G. Koster, Phys. Rev. B, **94**, 1498 (1954).

[118] C. M. Goringe, D. R. Bowler, and E. Hernandez, Rep. Prog. Phys., **60**, 1447 (1997).

[119] P. Lowdin, J. Chem. Phys., **18**, 365 (1950).

[120] E. I. Blount, in *Solid State Physics*, edited by F. Seitz and D. Turnbull (Academic, New York, 1962), Vol. 13.